IJC
International Journal of Cancer

Molecular characterization of long-term survivors of glioblastoma using genome- and transcriptome-wide profiling

Guido Reifenberger[1*], Ruthild G. Weber[2*], Vera Riehmer[2], Kerstin Kaulich[1], Edith Willscher[3], Henry Wirth[3], Jens Gietzelt[4], Bettina Hentschel[4], Manfred Westphal[5], Matthias Simon[6], Gabriele Schackert[7], Johannes Schramm[6], Jakob Matschke[8], Michael C. Sabel[9], Dorothee Gramatzki[10], Jörg Felsberg[1], Christian Hartmann[11,12], Joachim P. Steinbach[13,14], Uwe Schlegel[15], Wolfgang Wick[16], Bernhard Radlwimmer[17], Torsten Pietsch[18], Jörg C. Tonn[19], Andreas von Deimling[12], Hans Binder[3], Michael Weller[10,14+], and Markus Loeffler[4+]; for the German Glioma Network

[1] Department of Neuropathology, Heinrich Heine University, Düsseldorf, and German Cancer Consortium (DKTK), German Cancer Research Center (DKFZ), Heidelberg, Germany
[2] Department of Human Genetics, Hannover Medical School, Hannover, Germany
[3] Interdisciplinary Institute for Bioinformatics, University of Leipzig, Germany
[4] Institute for Medical Informatics, Statistics and Epidemiology, University of Leipzig, Germany
[5] Department of Neurosurgery, University Hospital Hamburg-Eppendorf, Hamburg, Germany
[6] Department of Neurosurgery, University of Bonn Medical School, Bonn, Germany
[7] Department of Neurosurgery, Technical University Dresden, Germany
[8] Institute of Neuropathology, University Hospital Hamburg-Eppendorf, Hamburg, Germany
[9] Department of Neurosurgery, Heinrich Heine University, Düsseldorf, Germany
[10] Department of Neurology, University Hospital Zurich, Switzerland
[11] Department of Neuropathology, Institute of Pathology, Hannover Medical School, Hannover, Germany
[12] Department of Neuropathology, Institute of Pathology, University Hospital Heidelberg, and Clinical Cooperation Unit Neuropathology, DKFZ, Heidelberg, Germany
[13] Dr. Senckenberg Institute of Neurooncology, University Hospital Frankfurt, Germany
[14] Department of General Neurology, University Hospital Tübingen, Germany
[15] Department of Neurology, University Hospital Knappschaftskrankenhaus Bochum-Langendreer, Bochum, Germany
[16] Department of Neurooncology, Neurology Clinic and National Center for Tumor Diseases, University Hospital Heidelberg, Germany
[17] Division of Molecular Genetics, DKFZ, Heidelberg, Germany
[18] Department of Neuropathology, University of Bonn Medical School, Bonn, Germany
[19] Department of Neurosurgery, Ludwig Maximilians University Munich, Germany

Cancer Genetics

Key words: array-based comparative genomic hybridization, gene expression profiles, glioblastoma, IDH1, integrative bioinformatics, long-term survival, MGMT

Abbreviations: CGH: comparative genomic hybridization; GGN: German Glioma Network; IDH: isocitrate dehydrogenase; KPS: Karnofsky performance score; MGMT: O^6-methylguanine DNA methyltransferase; OS: overall survival; PFS: progression-free survival; SOM: self-organising map; TMZ: temozolomide; WHO: World Health Organization

Additional Supporting Information may be found in the online version of this article.

Access to gene expression data: The gene expression data obtained in this study have been deposited in the gene expression omnibus (GEO) database at http://www.ncbi.nlm.nih.gov/geo/ (accession no. GSE53733).

Conflicts of interest: MiW has received research grants from Antisense Pharma, Merck Serono and Roche and honoraria for lectures or advisory boards from Antisense Pharma, Magforce, Merck Serono, MSD and Roche. JCT has received honoraria for lectures or advisory boards from Merck Serono, Medac and Roche. GR has received a research grant from Roche and honoraria for advisory boards from Merck Serono and Roche. US has received honoraria for lectures and advisory boards from Roche, Medac, GSK, Mundipharma and Sigma-tau. JS has been supported by a research grant from Merck Serono and received honoraria for advisory boards from Roche, Mundipharma and Medac. The other authors declare that they have no conflicts of interest.

*GR and RGW share first authorship.

+MW and ML share senior authorship.

Grant sponsor: German Cancer Aid (Deutsche Krebshilfe); **Grant number:** 70-3163-Wi 3

DOI: 10.1002/ijc.28836

History: Received 27 Dec 2013; Accepted 21 Feb 2014; Online 11 Mar 2014

Correspondence to: Guido Reifenberger, Department of Neuropathology, Heinrich Heine University, Moorenstrasse 5, D-40225 Düsseldorf, Germany, Tel.: [49-211-8118660], Fax: +[49-211-8117804], E-mail: reifenberger@med.uni-duesseldorf.de

The prognosis of glioblastoma, the most malignant type of glioma, is still poor, with only a minority of patients showing long-term survival of more than three years after diagnosis. To elucidate the molecular aberrations in glioblastomas of long-term survivors, we performed genome- and/or transcriptome-wide molecular profiling of glioblastoma samples from 94 patients, including 28 long-term survivors with >36 months overall survival (OS), 20 short-term survivors with <12 months OS and 46 patients with intermediate OS. Integrative bioinformatic analyses were used to characterize molecular aberrations in the distinct survival groups considering established molecular markers such as *isocitrate dehydrogenase 1* or *2 (IDH1/2)* mutations, and *O^6-methylguanine DNA methyltransferase* (*MGMT*) promoter methylation. Patients with long-term survival were younger and more often had *IDH1/2*-mutant and *MGMT*-methylated tumors. Gene expression profiling revealed over-representation of a distinct (proneural-like) expression signature in long-term survivors that was linked to *IDH1/2* mutation. However, *IDH1/2*-wildtype glioblastomas from long-term survivors did not show distinct gene expression profiles and included proneural, classical and mesenchymal glioblastoma subtypes. Genomic imbalances also differed between *IDH1/2*-mutant and *IDH1/2*-wildtype tumors, but not between survival groups of *IDH1/2*-wildtype patients. Thus, our data support an important role for *MGMT* promoter methylation and *IDH1/2* mutation in glioblastoma long-term survival and corroborate the association of *IDH1/2* mutation with distinct genomic and transcriptional profiles. Importantly, however, *IDH1/2*-wildtype glioblastomas in our cohort of long-term survivors lacked distinctive DNA copy number changes and gene expression signatures, indicating that other factors might have been responsible for long survival in this particular subgroup of patients.

What's new?

Long-term survival of more than 3 years after the diagnosis of glioblastoma is a rare and poorly understood phenomenon. Here, the authors sought to elucidate the molecular aberrations in glioblastomas of long-term survivors. They demonstrate that gene expression changes and genomic imbalances in glioblastomas from long-term survivors are closely associated with IDH1/2 mutation, but not with IDH1/2-independent long-term survival. Moreover, they disclose that most gene signatures previously linked to long-term survival are indeed associated with IDH1/2 mutation and are not prognostic in patients with IDH1/2-wildtype tumors. The molecular basis of long-term survival with IDH1/2-wildtype glioblastoma remains to be resolved.

Glioblastoma is the most common glial brain tumor with an annual incidence above 3 per 100,000 population.[1] Despite multimodal therapy, including neurosurgical resection and radiotherapy with concomitant and adjuvant temozolomide (TMZ),[2] the overall prognosis of glioblastoma patients remains poor. According to population-based data, median overall survival (OS) is still below one year and long-term survival is rare.[3,4] In a prospective German Glioma Network (GGN) study of 301 glioblastoma patients, median OS was 12.5 months.[5] However, a minority of glioblastoma patients survives for more than 36 months and has been referred to as long-term survivors.[6] These patients are usually young, have a good initial Karnofsky performance score (KPS), and their tumors often exhibit *O^6-methylguanine DNA methyltransferase* (*MGMT*) promoter methylation and *isocitrate dehydrogenase 1* or *2* (*IDH1/2*) mutations.[6,7]

Glioblastomas can be divided into primary glioblastomas, which preferentially arise *de novo* in patients older than 60 years of age, and secondary glioblastomas, which develop by progression from pre-existing lower grade gliomas and typically manifest in patients before the age of 50 years.[8] These glioblastoma types show distinct genetic aberrations, with *IDH1/2* mutation being common in secondary but rare in primary glioblastomas.[9–11] Patients with *IDH1/2*-mutant glioblastomas show longer survival than patients with *IDH1/2*-wildtype tumors.[5,12] However, *IDH1/2*-wildtype glioblastomas of long-term survivors have been poorly defined at the molecular level.[7] Recent studies have associated altered retinoic acid signaling,[13] enhanced immune-related gene expression,[14] and distinct DNA methylation profiles with long-term survival.[15] Nevertheless, it remained unclear how the molecular changes observed in long-term survivors are related to established markers, in particular *IDH1/2* mutation and *MGMT* promoter methylation. Therefore, we employed large-scale genome- and transcriptome-based analyses to characterize genomic imbalances and gene expression signatures in glioblastoma long-term survivors stratified according to the *IDH1/2* status, thus allowing for the distinction of *IDH1/2* mutation-dependent and -independent molecular changes in this intriguing patient group.

Patient and Methods

Patients

The GGN is a prospective, noninterventional cohort study that involves eight clinical centers in Germany (www.gliomnetzwerk.de) and was supported by the German Cancer Aid from 2004 to 2012. All patients gave their written informed consent for participation in the GGN and its translational research projects. For this study, we screened >300 prospectively recruited patients with a histopathological reference diagnosis of glioblastoma, known KPS at diagnosis, information on extent of resection by early postoperative neuroimaging, available frozen tissue specimens from the initial operation and documented

clinical outcome. After tissue evaluation and determination of *IDH1/2* mutation and *MGMT* promoter methylation status, tumor samples from 94 patients representing three distinct survival groups were included in the study. These included all long-term survivors from our database who had an OS of 36 months or more (Group A), as well as representative samples of two patient groups with short-term survival (Group B) or intermediate survival (Group C). Short-term survivors (Group B) had an OS of less than 12 months, with death due to tumor progression. Group C patients had intermediate survival and death in these patients had to be tumor-related. Likewise, the subpopulation of 79 patients with *IDH1/2*-wildtype tumors was subdivided into Group A^{wt}, Group B^{wt} and Group C^{wt}.

Central reference pathology

All tumors were subjected to central pathology review at the Brain Tumor Reference Center of the German Society of Neuropathology and Neuroanatomy (T.P.) and classified according to the World Health Organization classification of tumors of the central nervous system.[16]

Nucleic acid extraction and analyses for IDH1/2 mutation and MGMT promoter methylation

All investigated tissues were from the primary operation and thus had not been subjected to any treatment before. Tumor samples were shock-frozen after resection and stored at −80°C. Only specimens with a histologically estimated tumor cell content of 80% or more were used for molecular analyses. DNA and RNA were extracted by ultracentrifugation.[17] Analyses for *IDH1* and *IDH2* mutation were performed either by Sanger sequencing or pyrosequencing.[18,19] *MGMT* promoter methylation was determined by methylation-specific polymerase chain reaction.[20]

Affymetrix gene chip analyses

Transcriptome-wide changes in gene expression were determined by hybridization to Affymetrix Gene Chip® Human Genome U133 Plus 2.0 arrays (Affymetrix, Santa Clara, CA). Sample preparation was done with 2.5 μg total-RNA using the One Cycle Target Labelling and Controls kit (Affymetrix). Hybridizations were performed at the Center for Biological and Medical Research at Heinrich Heine University Düsseldorf. In total, 70 of the 94 tumors (23 Group A, 16 Group B and 31 Group C) were successfully analyzed.

Array-based comparative genomic hybridization (array-CGH) analyses

Eighty-nine of the 94 tumors were investigated by array-CGH using microarrays carrying 10,000 large insert clones with an average resolution of better than 0.5 Mb. Array assembly, hybridization and analysis were performed as described.[21]

Statistical and bioinformatical analyses

Gene expression was analyzed after data reduction to metagenes using self-organizing map (SOM) machine learning, which aggregates gene expression patterns of more than 20,000 genes into 2,500 "metagenes." These can be arranged in an intuitive quadratic mosaic portrait on a 50 × 50 grid using similarities. Each tile on this grid refers to one metagene collecting information on a variety of genes with correlated behavior across the data set.[22] Each metagene thus describes an expression profile of a microcluster of genes. Each tumor is characterized by the expression values of 2,500 metagenes that are visualized as expression landscape by color coding. Metagene-based clustering, visualization and downstream analysis of expression data was performed with the program OpoSOM after hook calibration of the raw data, quantile normalization and centralization in log10-scale (see Supporting Information Methods). In addition, we performed pairwise testing between groups of samples using moderate t-testing as implemented in the Linear Models for Microarray Data package.[23] For array-CGH evaluation, we used an established segmentation process to detect recurrent gains and losses. Data preprocessing and analysis were performed using aCGHPipeline.[24] Associations between different molecular parameters or patient groups were analyzed by Fisher's exact test using IBM SPSS Statistics Version 20.

Results

Patient characteristics

Supporting Information Table S1 summarizes the clinical characteristics of our patient population. Group A patients (long-term survivors) were younger than Group B (short-term survivors) and Group C patients (intermediate survival; $p = 0.02$). There were no differences in gender, KPS or extent of resection at initial surgery between the groups. *MGMT* promoter-methylated tumors ($p < 0.001$) and *IDH1/2*-mutant tumors ($p < 0.001$) were more common in group A. All Group B and most Groups A and C patients received radiotherapy plus TMZ as first-line therapy. PFS was profoundly longer in Group A than in the other groups ($p < 0.001$). Groups A and C patients received salvage therapies more often than Group B patients. The subgroup of 79 patients with *IDH1/2*-wildtype glioblastomas was accordingly divided into three distinct survival groups (Group A^{wt}, Group B^{wt} and Group C^{wt}) and analyzed independently (Supporting Information Table S2). Here, there were no differences in median age at diagnosis ($p = 0.303$). *MGMT* promoter-methylated tumors were more common in Group A^{wt} ($p = 0.002$).

Glioblastomas from long-term survivors carry distinct expression profiles that are linked to IDH1/2 mutation

Gene expression data were evaluated by SOM analysis, which allowed for the generation of individual expression maps, as well as mean portraits for groups of tumors and difference maps between tumor groups (Supporting Information Figs. S1, S2 and S4). Unsupervised clustering of the correlation matrix identified two major clusters: one included all *IDH1/2*-mutant and a minor fraction of the *IDH1/2*-wildtype tumors while the other one consisted exclusively of *IDH1/2*-

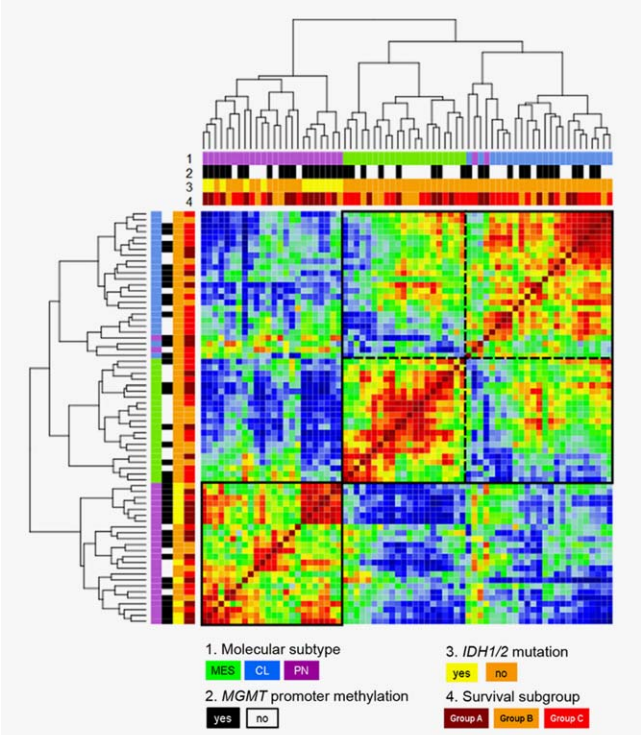

Figure 1. Results of gene expression profiling using unsupervised clustering. Shown is a pairwise correlation matrix based on SOM analysis of 70 glioblastomas. Strong positive or negative correlation is shown in dark red or blue, respectively, and intermediate levels are shown in green. The major cluster on the left includes all *IDH1/2*-mutant and a subset of the *IDH1/2*-wildtype tumors with proneural gene expression profiles. The large cluster on the right consists exclusively of *IDH1/2*-wildtype tumors with mostly classical or mesenchymal profiles.

wildtype tumors (Fig. 1). Tumors from long-term survivors (Group A) were enriched in the first cluster, as were tumors with *MGMT* promoter methylation. When relating our results to published gene expression signatures,[25] this cluster comprised exclusively glioblastomas with proneural signatures while the second cluster included tumors with classical, mesenchymal or proneural signatures (Fig. 1). Supporting Information Figure S3 provides a correlation network placing the individual tumors next to each other according to their highest mutual correlation between their SOM expression portraits. Using supervised analyses, we were able to identify a few genes that were differentially expressed between Group A and Group B tumors (Fig. 2*a* and Supporting Information Table S3). However, differential gene expression was much more prominent between *IDH1/2*-mutant and -wildtype glioblastomas (Fig. 2*b* and Supporting Information Table S4).

IDH1/2-wildtype glioblastomas from long-term survivors do not demonstrate distinct gene expression profiles

When performing unsupervised analysis of the 58 *IDH1/2*-wildtype glioblastomas (14 Group A^{wt}, 15 Group B^{wt} and 29 Group C^{wt}), we could not distinguish the different survival groups (Fig. 3*a*). Supervised comparison of Group A^{wt} versus Group B^{wt} patients suggested several differentially expressed genes (Supporting Information Table S5). However, significance for these genes disappeared after correction for multiple testing, and SOM analyses did not reveal differential expression profiles (Fig. 3*b*; Supporting Information Figs. S4 and S5). Hence, among *IDH1/2*-wildtype glioblastoma patients, long-term survivors (Group A^{wt}) could not be distinguished from patients with short-term (Group B^{wt}) or intermediate (Group C^{wt}) survival based on gene expression profiles.

Relationship between transcriptome-based molecular subtypes and survival groups

We also related gene expression in our cohort to the previously delineated neural, proneural, classical and mesenchymal glioblastoma subtypes.[25] While none of the tumors of our series displayed a neural expression profile, proneural, classical and mesenchymal signatures were detected in 26, 23 and 21 cases, respectively. Within each of the three subtypes, we reordered the correlation matrix according to survival groups. Figure 4 shows that each molecular subtype contains tumors from each survival group, with a trend for long-term survivors being more common in the proneural group ($p = 0.193$) that contained all *IDH1/2*-mutant tumors. However, this trend disappeared when only *IDH1/2*-wildtype tumors were considered ($p = 0.941$).

MGMT promoter methylation is common in long-term survivors but not linked to distinct expression profiles

MGMT promoter methylation was more common in Group A, that is, was detected in 20/23 tumors (9/9 *IDH1/2*-mutant and 11/14 *IDH1/2*-wildtype tumors), as opposed to 7/16 tumors in Group B and 13/31 tumors in Group C ($p = 0.002$). However, *IDH1/2*-wildtype glioblastomas with versus without *MGMT* promoter methylation did not demonstrate distinct expression profiles (Supporting Information Fig. S6A). Group-wise comparison of *MGMT* promoter-methylated Group A^{wt} versus Group B^{wt} or Group C^{wt} tumors did not detect distinctive gene signatures (Supporting Information Fig. S6B).

Genomic aberration profiles in glioblastomas are linked to IDH1/2 mutation status rather than long-term versus short-term survival

Unsupervised analysis of array-CGH data revealed several clusters of tumors, with most *IDH1/2*-wildtype glioblastomas harboring gains of chromosome 7, losses of 9p and chromosome 10, as well as additional gains of chromosomes 19 and 20 and/or losses on chromosomal arms 13q or 22q in about half of the cases each (Fig. 5*a*). Supervised comparison of genomic imbalances according to survival groups revealed these typical glioblastoma-associated alterations in a subset of Group A, as well as most Group B and Group C tumors (Fig. 5*b*). Genomic imbalances in *IDH1/2* mutant tumors

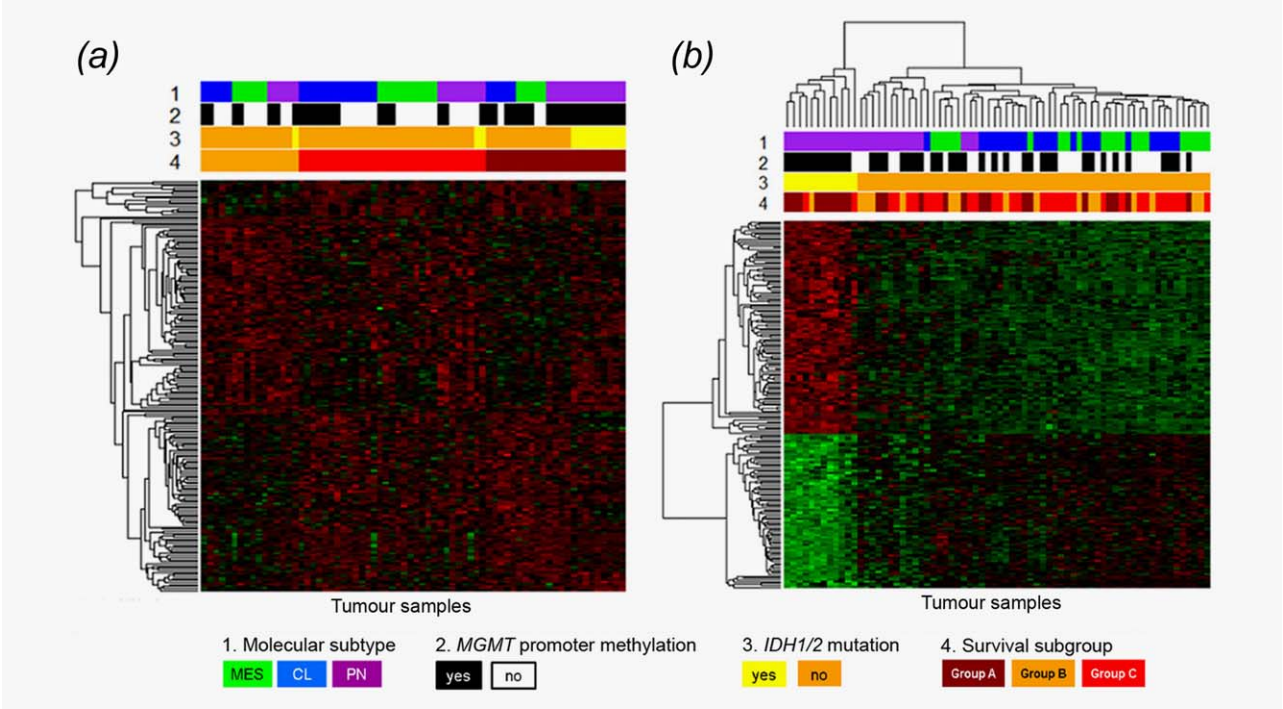

Figure 2. (*a*) Gene expression heatmap of all 70 tumors based on differentially expressed genes obtained by supervised comparison of Group A versus Group B tumors. Note relatively weak differences in gene expression between Group A tumors and tumors of the other two survival groups. (*b*) Gene expression heatmap obtained by unsupervised comparison of genes differentially expressed in *IDH1/2*-mutant versus-wildtype tumors. The heatmaps indicate high or low expression levels as green or red colors, respectively.

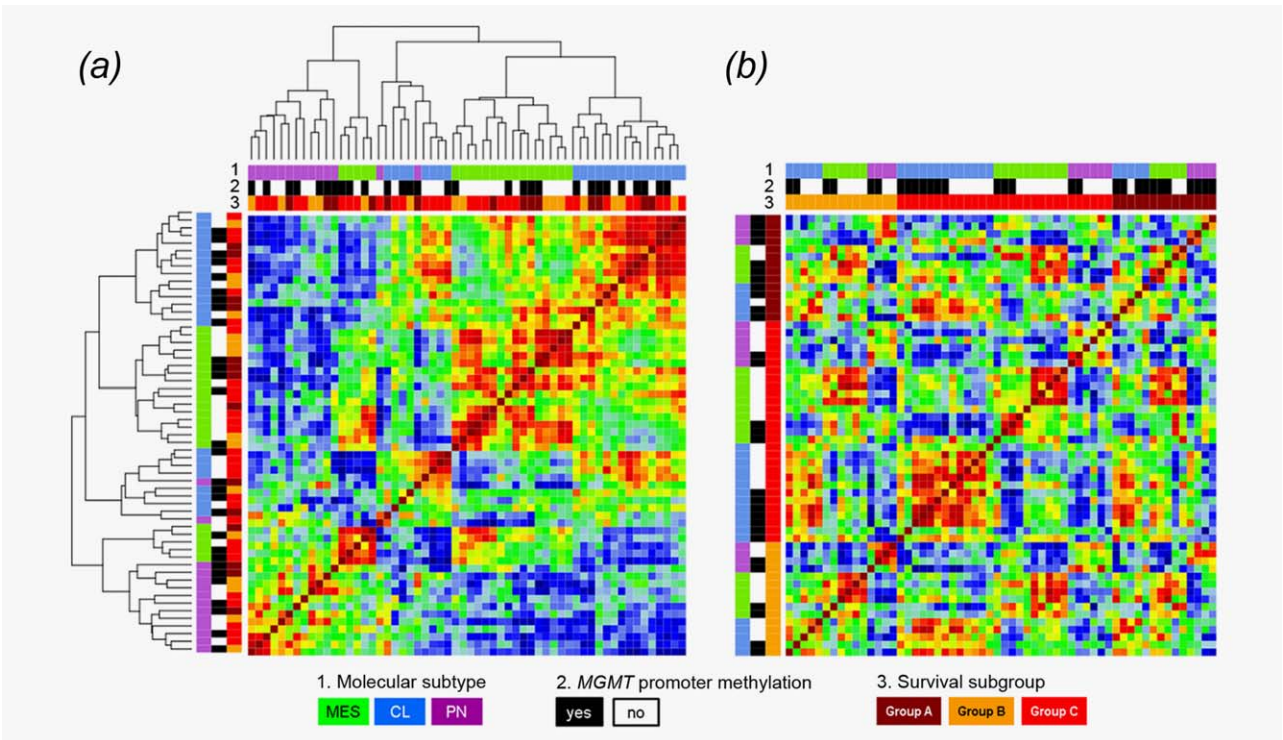

Figure 3. Results of gene expression profiling in the subgroup of *IDH1/2*-wildtype glioblastomas illustrated in pairwise correlation matrices. (*a*) Unsupervised clustering of the correlation matrix based on SOM analysis of all 58 *IDH1/2*-wildtype glioblastomas. Note that survival groups, molecular subtypes and *MGMT* promoter methylation are all widely distributed across all subclusters. (*b*) Gene expression matrix obtained by supervised comparison of Group A^{wt} versus Group B^{wt} and Group C^{wt} tumors based on SOM analysis. Note that the three survival groups do not demonstrate distinct expression profiles.

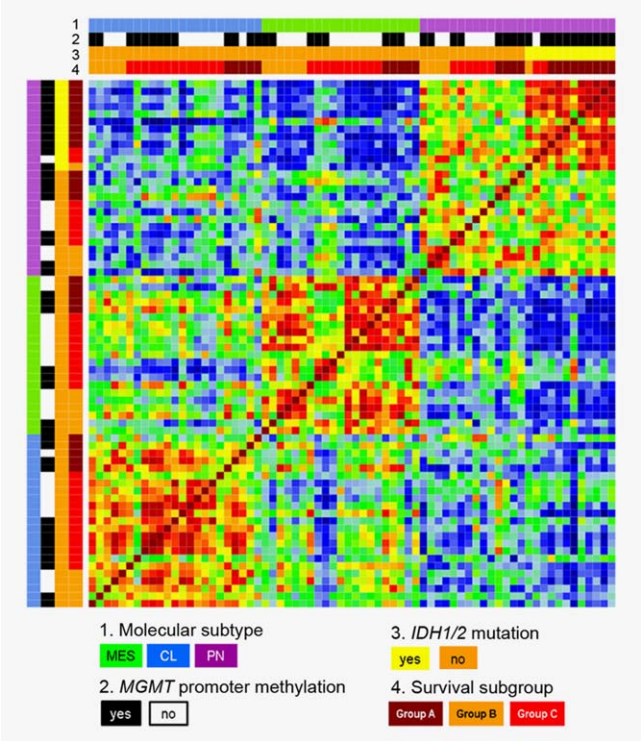

Figure 4. Results of expression profiling stratified according to molecular glioblastoma subtypes. The supervised pairwise correlation matrix shows that the distinct survival subgroups are distributed over all three molecular subtypes (classical, mesenchymal and proneural). The proneural subgroup is enriched for Group A as well as *IDH1/2*-mutant and *MGMT* promoter-methylated tumors.

were more widely distributed over different chromosomes (Figs. 5*b* and 6). Losses on 9p, 10 and 13q were also frequent while gains on 7, 19 or 20 were less common. Four tumors had combined losses on 1p and 19q. Clinical and histological review confirmed that these were primary glioblastomas without a history of preexisting lower grade glioma; however, three of them displayed an oligodendroglial tumor component. Comparison of gene expression profiles in the four 1p/19q-deleted and *IDH1/2*-mutant tumors with the eight 1p/19q-intact and *IDH1/2*-mutant tumors did not detect significant expression differences (Supporting Information Fig. S6C). Figure 6 shows frequency plots of genomic imbalances identified in the distinct survival groups of *IDH1/2*-wildtype glioblastoma patients and the group of patients with *IDH1/2*-mutant tumors, including 10 long-term survivors. Genomic profiles differed between *IDH1/2*-mutant and *IDH1/2*-wildtype glioblastomas, but were similar in the three *IDH1/2*-wildtype survival groups. Supporting Information Table S6 provides an overview of selected gene alterations detected by array-CGH and their relationship to the survival groups. Again, there was no over- or under-representation of any DNA copy number change in Group A^{wt} patients as compared with the *IDH1/2*-wildtype groups with shorter survival. In contrast, aberrations of several genes occurred at different frequencies in *IDH1/2*-wildtype versus *IDH1/2*-mutant tumors.

Combined analyses of genomic and expression data

Combined analyses of genomic and transcriptomic data revealed that mesenchymal and classical glioblastoma subtypes mostly carried the typical primary glioblastoma pattern of genomic imbalances, for example, gains on chromosome 7, 19 and 20, as well as losses on 9p, 10, 13q and 22q, while proneural glioblastomas showed more heterogeneous CGH patterns (Supporting Information Fig. 7). In addition, we found a number of cis-regulatory gene dosage effects on expression that were similar among the *IDH1/2*-wildtype survival groups but distinct in the *IDH1/2*-mutant group (Supporting Information Fig. 8). For example, the frequent monosomy of chromosome 10 in *IDH1/2*-wildtype tumors resulted in reduced expression of many genes on this chromosome, while expression of these genes was higher in *IDH1/2*-mutant tumors that less frequently demonstrate complete chromosome 10 losses. Similarly, the frequent chromosome 7 gain in *IDH1/2*-wildtype glioblastomas was associated with increased expression of genes located on this chromosome.

Evaluation of published prognostic gene signatures

Several studies reported on gene signatures associated with glioblastoma long-term survival. Mapping of these signatures to our data set uniformly showed preferential associations with the *IDH1/2* mutation status but not with *IDH1/2*-independent survival (Supporting Information Fig. 9). For example, we found the signatures related to immune function or innate immunity reported for long-term survivors[14] to be associated with *IDH1/2* mutation but not with *IDH1/2*-independent long-term survival. The prognostic signature developed by Nutt et al.[26] using expression profiling of anaplastic oligodendrogliomas versus primary glioblastomas was also linked to *IDH1/2* mutation but not to survival in *IDH1/2*-wildtype patients. The 42-probe set signature found in a subgroup of glioblastoma patients with longer survival in The Cancer Genome Atlas (TCGA) cohort[27] distinguished Group A from Group B patients in our series, but also was strongly linked to the *IDH1/2* status, and lacked differential expression between the *IDH1/2*-wildtype survival groups. We also evaluated gene methylation data previously linked to glioblastoma long-term survival[15] by transforming the differentially methylated genes into gene expression signatures that were mapped to our SOM data. Again, differential expression of reported prognostic methylation profiles closely associated with *IDH1/2* mutation but not with long-term survival in *IDH1/2*-wildtype patients (Supporting Information Fig. 10).

Validation experiments using TCGA data

To validate our findings in an independent data set, we evaluated gene expression profiles in relation to patient survival in a subset of 153 glioblastomas of the TCGA data set. From this cohort, we selected 101 patients whose tumors were *IDH1*-wildtype or showed mesenchymal or classical gene

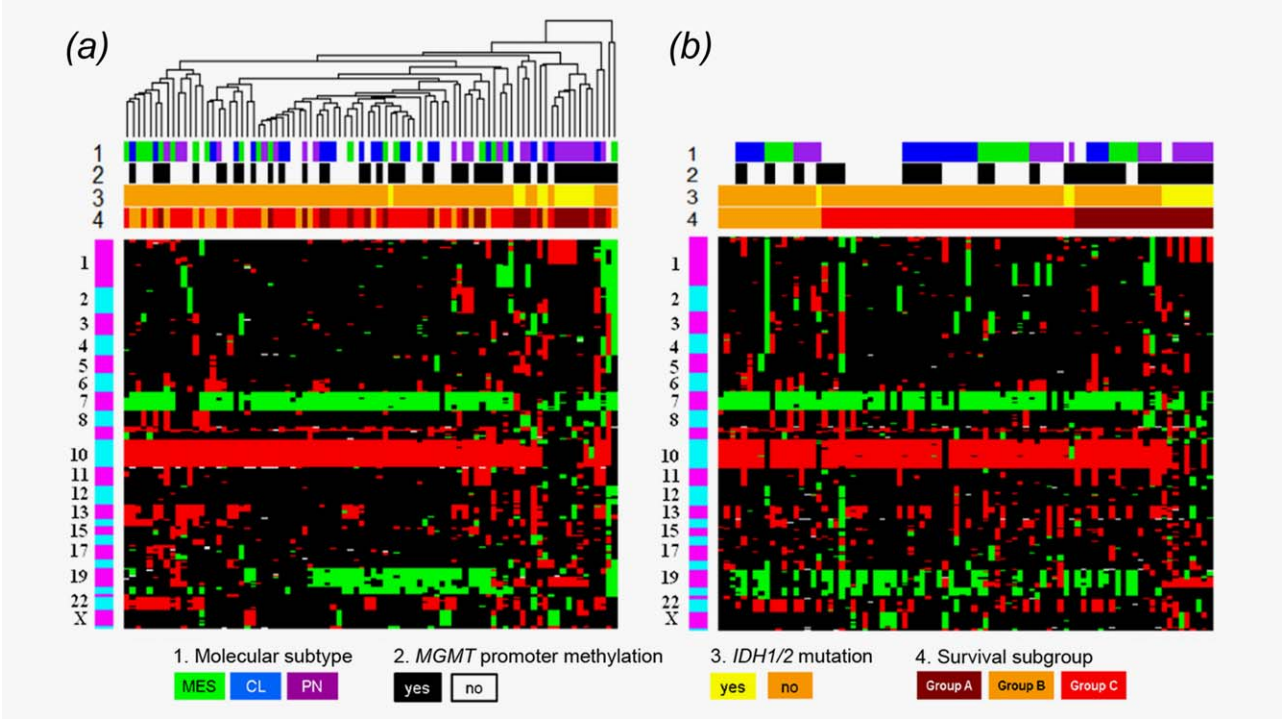

Figure 5. Summary of genomic aberration profiles detected by array-CGH in 89 glioblastomas. (*a*) The heatmap shows results of an unsupervised clustering of the array-CGH results (gains indicated in green, losses in red). Survival groups, *IDH1/2* mutation status, *MGMT* promoter methylation status and molecular subtype are illustrated on top of the heatmap. Several subclusters are evident, with most *IDH1/2*-mutant tumors forming a cluster separate from the bulk of *IDH1/2*-wildtype tumors. The latter are mainly characterized by gains of chromosome 7 and losses of chromosome 10 and chromosome arm 9p. In addition, gains of chromosomes 19 and 20 as well as losses of chromosomes 13 and 22 q are found in larger subgroups of tumors. The *IDH1/2*-mutant tumors show more heterogeneous aberration patterns. Note that Group A patients are widely distributed over all clusters with enrichment in the *IDH1/2*-mutant and *MGMT* promoter-methylated tumors on the right hand side. (*b*) Results obtained by supervised clustering of array-CGH data based on survival subgroups.

expression profiles that are exclusive to *IDH1* mutation (Supporting Information Table S7; Supporting Information Fig. 11). This TCGA cohort included 9 patients with OS of 36 months or more, 48 patients with OS of less than 12 months and 44 patients with intermediate OS. The respective mRNA expression data were analyzed with our SOM pipeline, which revealed no distinctive gene expression profile in the group of *IDH1/2*-wildtype glioblastomas of long-term survivors (Supporting Information Fig. S11), thus validating the findings in the GGN cohort.

Discussion

Long-term survival of glioblastoma is a rare and poorly understood phenomenon. While socioeconomic, environmental and occupational factors appear not to play major roles, certain molecular aberrations, in particular *MGMT* promoter methylation and *IDH1/2* mutation, are more common in long-term survivors than in unselected patients.[6,7] Previous studies revealed distinct gene expression profiles and characteristic changes in DNA methylation in glioblastomas from long-term survivors.[13–15] Collectively, these data suggest marked differences in tumor biology as a major factor underlying glioblastoma long-term survival. Therefore, we investigated a clinically well-characterized cohort of glioblastoma patients with long-term survival of more than 3 years, short-term or intermediate OS, all treated according to the current standard of care. The tumors were subjected to genome- and transcriptome-wide profiling as well as focused analyses for *IDH1/2* mutation and *MGMT* promoter methylation. Based on this extensive molecular evaluation, we confirm the overrepresentation of tumors with *MGMT* promoter methylation and *IDH1/2* mutation among glioblastomas from long-term survivors. A minor subset of *IDH1/2*-mutant glioblastomas from our present long-term survivor cohort additionally carried 1p/19q deletions, although our previous analyses of formalin-fixed and paraffin-embedded tissue specimens from larger cohorts did not demonstrate an increased incidence of 1p/19q deletion in long-term survivors.[6,7] We also demonstrate that *IDH1/2* mutation in glioblastomas with long-term survival is associated with distinct genomic and transcriptomic profiles,[28,29] the latter likely being associated with *IDH1/2* mutation-associated global changes in DNA methylation known as glioma CpG island methylator phenotype (G-CIMP).[28,30] However, our findings also indicate that in patients with *IDH1/2*-wildtype glioblastoma, survival of longer than 3 years does not appear to be linked to distinctive DNA copy number changes or gene expression profiles.

Importantly, albeit somewhat disappointing, we additionally disclose various prognostic gene signatures previously

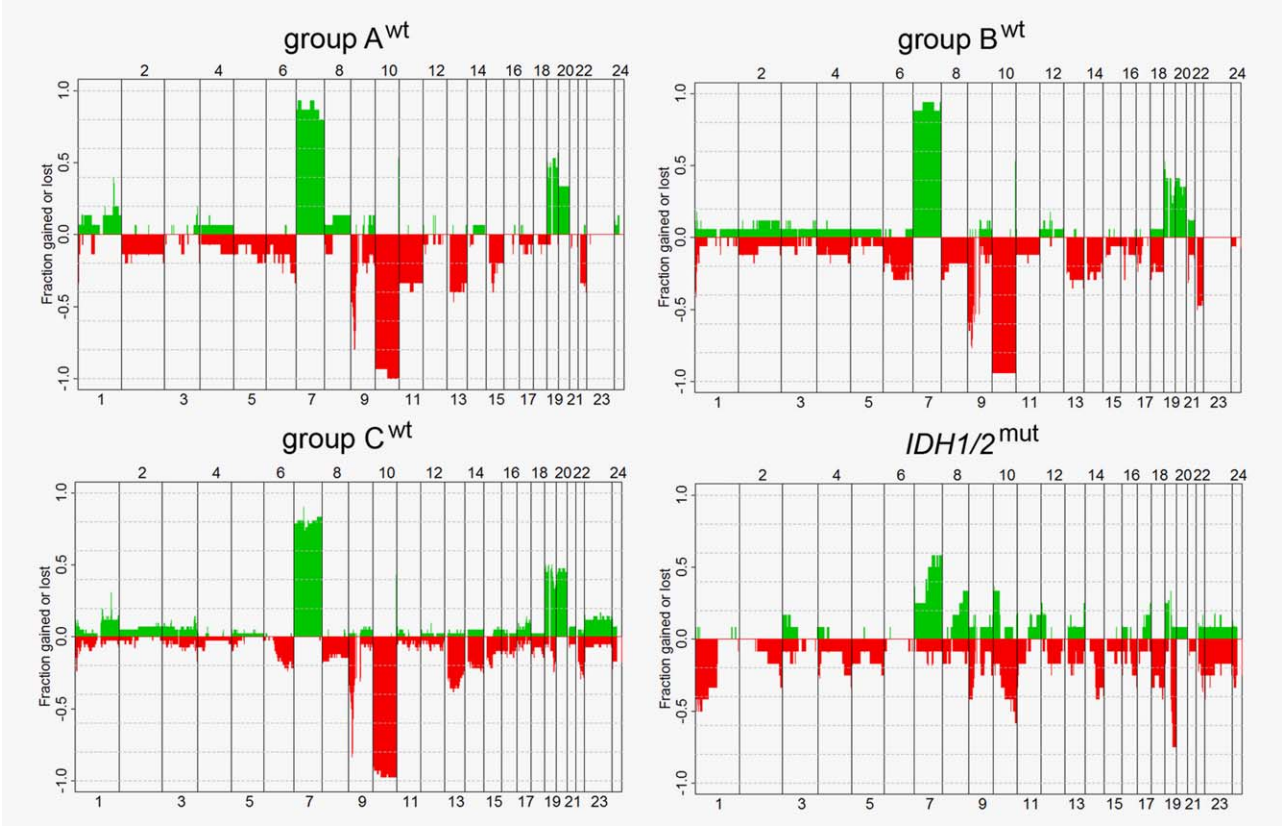

Figure 6. Patterns of genomic imbalances in glioblastomas according to survival groups and *IDH1/2* mutation status. Frequency plots of genomic imbalances detected in the three distinct survival groups of *IDH1/2*-wildtype glioblastoma patients (Group A^{wt}, Group B^{wt} and Group C^{wt}), as well as the group of patients with *IDH1/2*-mutant tumors (*IDH1/2*^{mut}). Note similar patterns of genomic imbalances in the three *IDH1/2*-wildtype groups but distinct patterns in the *IDH1/2*-mutant group, including 1p/19q deletions in a fraction of cases. The individual chromosomes are listed at the bottom of each plot. Copy number gains are indicated in green and losses in red.

reported as characteristic of glioblastoma long-term survivors as being essentially related to the *IDH1/2* mutation status, but without predictive value independent from *IDH1/2* mutation in our patient cohort. For example, using microarray-based profiling of 26 high-grade gliomas, including three glioblastomas from patients with >5 years OS, Donson and co-workers[14] found an increased expression of immune function-related genes in tumors of long-term survivors, including a notable T-cell signature that was present within this prognostic immune gene set. However, the authors did not stratify their patients according to the *IDH1/2* mutation status. Application of their signature to our data set demonstrated an association with *IDH1/2* mutation but not with *IDH1/2*-independent long-term survival. Similarly, the prognostic gene signature reported by Nutt et al.,[26] which originated from the comparison of anaplastic oligodendrogliomas, which likely were *IDH1/2*-mutant, with primary glioblastomas, which likely were *IDH1/2*-wildtype, revealed an association with *IDH1/2* mutation but not with survival in *IDH1/2*-wildtype patients. Also, the 42-probe set signature recently reported by Kim et al.[27] revealed a clear association with *IDH1/2* mutation and no differential expression between the *IDH1/2*-wildtype survival groups of our cohort (see Supporting Information Results and Supporting Information Fig. 10 for further results obtained for additional prognostic signatures mapped to our data set). Moreover, analyses of prognostic methylation signatures reported as being linked to *IDH1/2* mutation[30] or long-term survival of glioblastoma[15] did not reveal an association with long-term survival in our patients with *IDH1/2*-wildtype glioblastoma. In line with these findings, we also did not identify a distinctive gene expression profile in *IDH1/2*-wildtype glioblastomas from long-term survivors in an independent validation cohort of TCGA patients. Our findings are further supported by the most recent TCGA publication.[31] Based on mRNA profiling of more than 500 glioblastoma patients, this study confirmed a prognostic role of the proneural expression signature only for patients whose tumors showed the G-CIMP phenotype, which is closely linked to *IDH1/2* mutation, while none of the four expression signatures (proneural, neural, mesenchymal and classic) was prognostic in patients whose tumors lacked G-CIMP, that is, the vast majority of primary, *IDH1/2* wild-type glioblastoma patients.[31]

A potential weakness of our study is the relatively small number of patients in the distinct survival groups, mainly due to the rarity of available frozen tumor samples from long-term survivors. In addition, the combination of

radiotherapy with TMZ chemotherapy has led to an increased percentage of glioblastoma patients surviving for three years or longer in clinical trial populations, as indicated by the recent finding that ~20% of the patients in the RTOG 0525 trial survived for 36 months or longer.[32] Therefore, one may speculate that the arbitrary >36-months cut-off originally proposed to define long-term survival of glioblastoma patients[6] may no longer be suited for a clear molecular distinction between long-term and short-term survivors. However, an extended survival cut-off, for example, survival of >5 years after diagnosis,[14] further reduces the number of patients with available frozen tissue samples. For example, the large TCGA glioblastoma cohort of more than 500 patients[31] includes only six patients who survived for longer than five years after diagnosis. Thus, molecular characterization of a reasonable number of glioblastoma patients surviving beyond five years after diagnosis requires access to huge patients cohorts that may only be recruited in large international collaborations.

In summary, *IDH1/2* mutation is associated with distinct genomic and transcriptomic changes that together define a molecular subtype of glioblastoma with better prognosis and increased likelihood for long-term survival. *MGMT* promoter methylation also is more common in long-term survivors treated according to the current standard of care, including both patients with *IDH1/2*-mutant and *IDH1/2*-wildtype tumors. However, survival of three years or more with *IDH1/2*-wildtype glioblastoma was not linked to distinct mRNA expression profiles or genomic imbalances detectable by the microarray-based approaches used in our study. Further studies thus should focus on the analysis of subtler genetic/epigenetic alterations using whole genome/epigenome sequencing, preferentially in patients with more than five years OS. In addition, post-transcriptional/proteomic alterations might be associated with *IDH1/2*-independent long-term survival. Finally, the characterization of to date poorly understood host-related factors, such as differences in the anti-tumor immune response, appears to be an attractive future research field.

Acknowledgements

The authors greatly acknowledge the support by the staff at the German Glioma Network centers. Thorsten Wachtmeister, Genomics and Transcriptomics Laboratory, Center for Biological and Medical Research, Heinrich Heine University Düsseldorf, is greatly acknowledged for his support of the Affymetrix chip hybridization experiments. Validation data sets were retrieved from The Cancer Genome Atlas (TCGA) database established by the NCI and NHGRI (http://cancergenome.nih.gov/).

Author's contributions

GR, MiW and ML conceived this study within the German Glioma Network. JF, CH, KK, VR, BR, AvD, RGW and GR contributed to the molecular analyses. HB, HW, ML, RGW and GR developed the strategy for bioinformatic data evaluation. HW wrote the R-programs used for SOM analyses. EW and JG evaluated gene expression data and prepared the figures. BH carried out statistical analyses. TP reviewed all histological specimens. MaW, MS, GS, JSch, JM, MCS, DG, JPS, US, WW and JCT contributed patient samples and clinical data. Manuscript and online supplement were written by GR, RGW, HB, MiW and ML, with support from all authors. The final version of the article was reviewed and approved by all authors.

References

1. Dolecek TA, Propp JM, Stroup NE, et al. CBTRUS statistical report: primary brain and central nervous system tumors diagnosed in the United States in 2005-2009. *Neuro Oncol* 2012;14 Suppl 5:v1–49.
2. Stupp R, Mason WP, van den Bent MJ, et al. Radiotherapy plus concomitant and adjuvant temozolomide for glioblastoma. *N Engl J Med* 2005;352:987–96.
3. Johnson DR, O'Neill BP. Glioblastoma survival in the United States before and during the temozolomide era. *J Neurooncol* 2012;107:359–64.
4. Rønning PA, Helseth E, Meling TR, et al. A population-based study on the effect of temozolomide in the treatment of glioblastoma multiforme. *Neuro Oncol* 2012;14:1178–84.
5. Weller M, Felsberg J, Hartmann C, et al. Molecular predictors of progression-free and overall survival in patients with newly diagnosed glioblastoma. A prospective translational study of the German Glioma Network. *J Clin Oncol* 2009;27:5743–50.
6. Krex D, Klink B, Hartmann C, et al. Long-term survival with glioblastoma multiforme. *Brain* 2007;130:2596–606.
7. Hartmann C, Hentschel B, Simon M, et al. Long-term survival in primary glioblastoma with versus without isocitrate dehydrogenase mutations. *Clin Cancer Res* 2013;19:5146-5157.
8. Ohgaki H, Kleihues P. The definition of primary and secondary glioblastoma. *Clin Cancer Res* 2013;19:764–72.
9. Balss J, Meyer J, Mueller W, et al. Analysis of the IDH1 codon 132 mutation in brain tumors. *Acta Neuropathol* 2008;116:597–602.
10. Parsons DW, Jones S, Zhang X, et al. An integrated genomic analysis of human glioblastoma multiforme. *Science* 2008;321:1807–12.
11. Yan H, Parsons DW, Jin G, et al. IDH1 and IDH2 mutations in gliomas. *N Engl J Med* 2009;360:765–73.
12. Sanson M, Marie Y, Paris S, et al. Isocitrate dehydrogenase 1 codon 132 mutation is an important prognostic biomarker in gliomas. *J Clin Oncol* 2009;27:4150–4.
13. Barbus S, Tews B, Karra D, et al. Differential retinoic acid signaling in tumors of long- and short-term glioblastoma survivors. *J Natl Cancer Inst* 2011;103:598–606.
14. Donson AM, Birks DK, Schittone SA, et al. Increased immune gene expression and immune cell infiltration in high-grade astrocytoma distinguish long-term from short-term survivors. *J Immunol* 2012;189:1920–7.
15. Shinawi T, Hill VK, Krex D, et al. DNA methylation profiles of long- and short-term glioblastoma survivors. *Epigenetics* 2013;8:149-56.
16. Kleihues P, Burger PC, Aldape K, et al. Glioblastoma. In: Louis DN, Ohgaki H, Wiestler OD, Cavanee WK, eds. WHO Classification of Tumours of the Central Nervous System. Lyon: IARC, 2007. 33–49.
17. van den Boom J, Wolter M, Kuick R, et al. Characterisation of gene expression profiles associated with glioma progression using oligonucleotide-based microarray analysis and real-time reverse transcription-polymerase chain reaction. *Am J Pathol* 2003;163:1033–43.
18. Felsberg J, Wolter M, Seul H, et al. Rapid and sensitive assessment of the IDH1 and IDH2 mutation status in cerebral gliomas based on DNA pyrosequencing. *Acta Neuropathol* 2010;119:501–7.
19. Hartmann C, Meyer J, Balss J, et al. Type and frequency of IDH1 and IDH2 mutations are related to astrocytic and oligodendroglial differentiation and age: a study of 1,010 diffuse gliomas. *Acta Neuropathol* 2009;118:469–74.
20. Felsberg J, Rapp M, Loeser S, et al. Prognostic significance of molecular markers and extent of

resection in primary glioblastoma patients. *Clin Cancer Res* 2009;15:6683–93.
21. Zielinski B, Gratias S, Toedt G, et al. Detection of chromosomal imbalances in retinoblastoma by matrix-based comparative genomic hybridization. *Genes Chromosomes Cancer* 2005;43: 294–301.
22. Wirth H, Löffler M, von Bergen M, et al. Expression cartography of human tissues using self organizing maps. *BMC Bioinformatics* 2011;12: 306.
23. Smyth GK. Linear models and empirical bayes methods for assessing differential expression in microarray experiments. *Stat Appl Genet Mol Biol* 2004;3:Article 3.
24. Kreuz M, Rosolowski M, Berger H, et al. Development and implementation of an analysis tool for array-based comparative genomic hybridization. *Methods Inf Med* 2007;46: 608–13.
25. Verhaak RG, Hoadley KA, Purdom E, et al. Integrated genomic analysis identifies clinically relevant subtypes of glioblastoma characterized by abnormalities in PDGFRA, IDH1, EGFR, and NF1. *Cancer Cell* 2010;17:98–110.
26. Nutt CL, Mani DR, Betensky RA, et al. Gene expression-based classification of malignant gliomas correlates better with survival than histological classification. *Cancer Res* 2003;63: 1602–7.
27. Kim YW, Koul D, Kim SH, et al. Identification of prognostic gene signatures of glioblastoma: a study based on TCGA data analysis. *Neuro Oncol* 2013;15:829-39.
28. Sturm D, Witt H, Hovestadt V, et al. Hotspot mutations in H3F3A and IDH1 define distinct epigenetic and biological subgroups of glioblastoma. *Cancer Cell* 2012;22:425–37.
29. Toedt G, Barbus S, Wolter M, et al. Molecular signatures classify astrocytic gliomas by IDH1 mutation status. *Int J Cancer* 2011;128: 1095–103.
30. Noushmehr H, Weisenberger DJ, Diefes K, et al. Identification of a CpG island methylator phenotype that defines a distinct subgroup of glioma. *Cancer Cell* 2010;17: 510–22.
31. Brennan CW, Verhaak RG, McKenna A, et al. The somatic genomic landscape of glioblastoma. *Cell* 2013;155:462-77.
32. Gilbert MR, Wang M, Aldape KD, et al. Dose-dense temozolomide for newly diagnosed glioblastoma: a randomized phase III clinical trial. *J Clin Oncol* 2013;31:4085-91.

Supplementary material

Molecular characterization of long-term survivors of glioblastoma using genome- and transcriptome-wide profiling analyses

Guido Reifenberger, MD, Ruthild G. Weber, MD, Vera Riehmer, Kerstin Kaulich, PhD, Edith Willscher, Henry Wirth, PhD, Jens Gietzelt, Bettina Hentschel, Manfred Westphal, MD, Matthias Simon, MD, Gabriele Schackert, MD, Johannes Schramm, MD, Jakob Matschke, MD, Michael C. Sabel, MD, Dorothee Gramatzki, MD, Jörg Felsberg, MD, Christian Hartmann, MD, Joachim Steinbach, MD, Uwe Schlegel, MD, Wolfgang Wick, MD, Bernhard Radlwimmer, PhD, Torsten Pietsch, MD, Jörg C. Tonn, MD, Andreas von Deimling, MD, Hans Binder, PhD, Michael Weller, MD, Markus Loeffler, MD, for the German Glioma Network

Supplementary methods

Self-Organizing Map (SOM) portraying, differential and similarity analyses

Pre-processing and calibration of microarray results: Raw probe intensities of Affymetrix microarrays were calibrated and summarized into one expression value per probe set using the hook method Binder et al.,[1,2] and then quantile-normalised and corrected for background-noise as described elsewhere.[3] The expression value of each gene was transformed into log10-scale and centered with respect to its mean value averaged over all samples investigated. A relative log-expression value of zero consequently indicates that the gene is expressed according to its mean expression value in the investigated sample, while positive or negative values refer to increased or reduced expression levels, respectively.

SOM training: The pre-processed expression data were used to train a self-organizing map (SOM). This translates the high-dimensional expression data given as N x M matrix (N: number of genes, M: number of samples) into a K x M matrix (K: number of so-called metagenes) of reduced dimensionality K<<N (N~ 20,000 and K~2,500). The rows define the expression profiles, i.e., the expression values of one gene in all samples, and the columns define the expression states or landscapes, i.e., the expression values of all genes in one sample. The K metagenes are arranged in a 50 x 50 two-dimensional quadratic grid. After appropriate initialisation,[4] their profiles are obtained via iterative machine learning using about 250,000 steps. In each step, the SOM algorithm distributes the genes over the grid so that each gene is associated with the metagene showing the most similar expression profile. In addition, it adapts the metagene profiles in small increments to the observed single gene profiles. In consequence, the resulting map becomes self-organised, which means that genes of similar profiles are clustered together either within one metagene or in simalar metagenes positioned in an adjacent location, whereas genes with distinct expression profiles localise in different regions of the map. The degree of similarity between metagenes decreases with increasing distance in the map. Importantly, each metagene serves as a representative prototype of a 'microcluster' of real genes with similar expression profiles. Analysis in metagene-space instead of real gene space is advantageous in several aspects: (i) effective and power-gaining in significance testing, (ii) representative, (iii) illustrative and intuitive, and (iv) no loss of information with respect to single gene properties.[3,4]

SOM staining: The expression state of each sample was visualised by color-coding the two-dimensional mosaic of metagenes according to their expression values in the respective sample.

Supplementary Figure 1 shows the gallery of gene expression SOM images of the 70 glioblastomas that were successfully evaluated in our study. Average subtype-specific portraits are calculated as the mean value of each relative metagene expression over all portraits of one group of tumors. To extract differential expression landscapes, we calculated difference maps between groups of tumors to visualise clusters of differentially up- or down-regulated genes. Log-fold change (logFC) and explicit significance metrics are used for color-coding (see below).

Expression modules: The SOM algorithm arranges similar metagene profiles in neighboured tiles of the map whereas less similar metagene profiles are located more distantly apart from each other. In consequence, neighboured metagenes tend to be colored similarly owing to their similar expression profiles showing a smooth texture with red and blue spot-like regions referring to clusters of over- and underexpressed metagenes, respectively. Metagenes from the same spot are co-expressed in the experimental series and thus refer to the same expression module. In contrast, genes from different, well-separated spots refer to distinct expression modules showing different expression profiles.

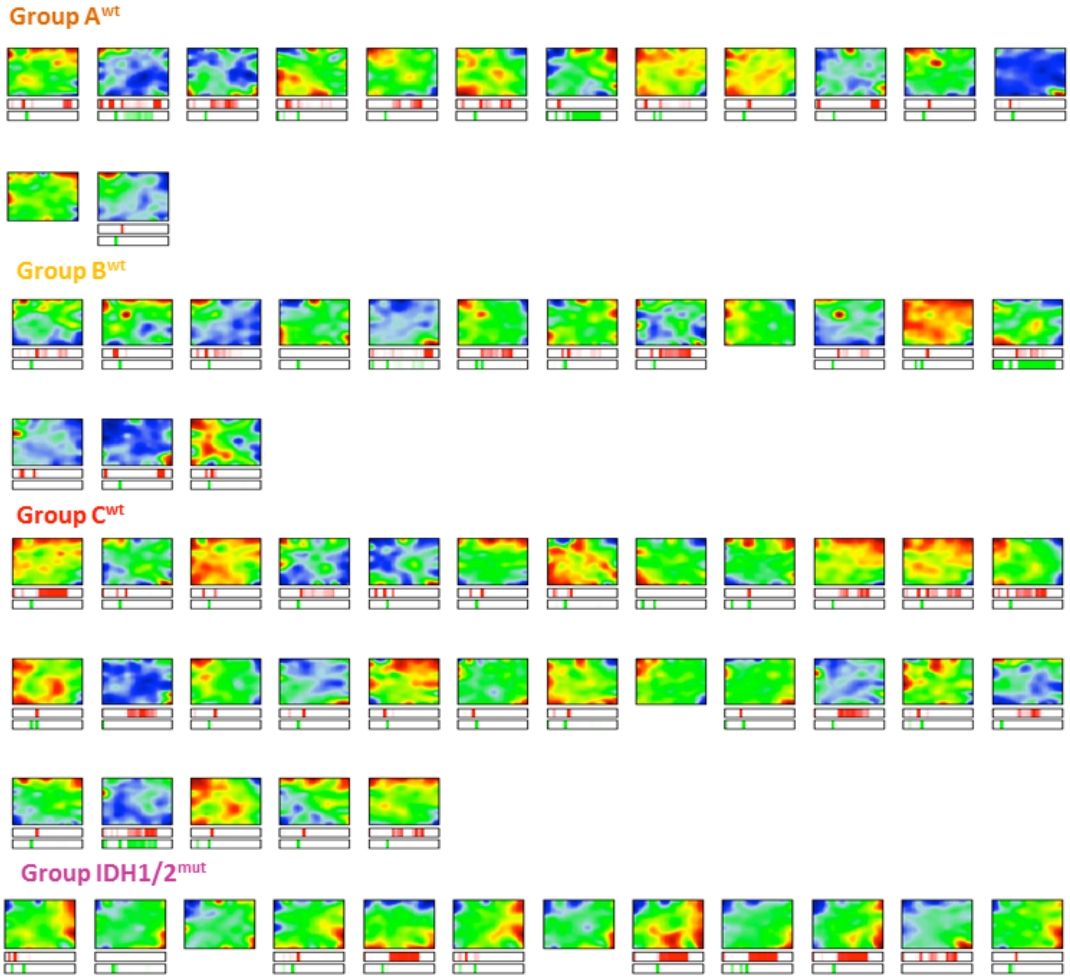

Supplementary Figure 1. Gallery of 70 SOM-images that portray the individual expression landscape of each tumor sample investigated in our study. Red and blue regions in the images refer to up-regulated or down-regulated genes, respectively. The two bars below each of the images visualise the respective CGH aberration patterns: Chromosomes are ordered from the left to the right from chromosome 1 to chromosome 22. Red and green marks in the bars denote copy number losses and gains, respectively. Samples are grouped according to their *IDH1/2* mutation status '*IDH1/2*^{wt}' for *IDH1/2* wildtype; '*IDH1/2*^{mut}' for *IDH1/2* mutant) and survival groups for *IDH1/2*^{wt} tumors (groups A, B and C). Note that *IDH1/2* mutation is typically associated with red and blue spots in the right lower and left upper corners of each map. In contrast, the *IDH1/2*^{wt} tumors show more heterogeneous spot patterns without clear preferences.

Gene set population maps and GSZ-profiles: Selected sets of genes taken from previous publications of independent analyses can be mapped into SOM space to characterize highly-populated clusters of genes. These gene set population maps can be color-coded regarding the number of genes from the set found in each of the tiles of the SOM. Genes found in the same cluster are co-expressed in terms of correlated expression profiles and they can be assumed to be functionally related according to the 'guilty-by-association' principle. In contrast, single genes outside such cluster regions do virtually not co-express with other genes in our data. Therefore, they can be regarded as candidates for false positive results. Gene set expression profiles are calculated in units of the gene set enrichment Z-score (GSZ-score) defined previously (see Wirth et al.[4] and the references cited therein). In this particular case, the sample-specific GSZ-profile is defined as the difference between the mean expression of all genes of the set in the sample selected and its mean value averaged over all samples divided by the respective standard deviation that considers the variance of the expression of the set members in the sample selected and of its mean value in all samples. GSZ-profiles are shown either as box or as bar plots, in which each box/bar refers to one group of samples/one individual sample.

Mean SOMs, differential SOM portraits and significance maps: To enable aggregate use of metagene information in pairwise comparisons of groups of samples, we calculated mean SOMs by averaging each metagene value over all members of the respective patient group. Difference SOM portraits were obtained by subtracting two SOM maps from groups of samples and color-coding of the mean differential expression between the groups for each metagene. The p-value for difference testing was then obtained for each metagene by randomization of the metagene values and resampling to obtain an appropriate null-distribution as reference. Consideration of the density distribution of the p-values of all metagenes allows for the estimation of the false discovery rate (fdr) for each metagene to control for the number of false positive discoveries in the multiple testing problem.[5] The p- and fdr-values were mapped into SOM-space to obtain the respective SOM-wide significance maps that color code the metagene-related p- and fdr-values, respectively. Significance of differential expression of selected gene sets between groups of samples was calculated by pairwise comparison of their GSZ-score and subsequent Mann-Whitney-U testing.

Sample similarity analysis and SOM-based correlation matrices: Sample similarity analysis establishes mutual relations between different samples. We compared the expression states characterized by the SOM portraits. This approach uses metagenes instead of single genes as the basal data, which has the advantage of improving the representativeness and resolution of the results.[3,4] Similarity between samples was estimated in terms of Pearson's correlation coefficient calculated between all metagene values in pairwise combinations of samples. The resulting SOM-based correlation structure was visualised using either pairwise correlation matrix (PCM) and correlation net (CN) representations (Supplementary Supplementary Figure **2**). The PCM labels positive and negative correlations in red and blue, respectively, using a quadratic grid with/or without K-means clustering of the samples to obtain unsupervised or supervised heatmaps, respectively. CN represents an unweighted graph connecting the nodes, i.e., the tumor samples, whose pairwise correlation coefficient exceeds a given threshold (r=0.5).

Program: We used the R-program 'oposSOM' for SOM-training and downstream analysis.[3] This program is available as R-package on CRAN repository (http://cran.r-project.org/).

Classification into glioblastoma expression subtypes using the SOM method

First, we trained a SOM using all individual patient data (**Supplementary Figure 1**). Then, classification of samples was performed as outlined in Supplementary Figure 2. Classifier genes for glioblastoma subtypes were taken from published data[6] and mapped into the SOM space. Each sample portrait was then compared with the set of these prototypic class maps chosen and assigned to the class of closest similarity using the Euclidian distance as criterion. New class maps were obtained as mean SOM portraits averaged over all sample portraits of each class. These three steps, comparison with sample portraits, classification and calculation of newly averaged maps were repeated until the algorithm settled down, i.e. no samples were rearranged between the classes anymore. Robustness of

classification of each sample was estimated by bootstrapping. The method randomly selects a subset of samples from all samples available and performs K-means clustering to assign their class membership. The percentage of realizations with proper class assignment agreeing with the original assignment then estimated the robustness of classification.

Differential gene expression analysis using LIMMA

Differential gene expression analysis was performed by using the moderate-t-test of the LIMMA package with the individual variance of each gene being shrunken towards a global variance. The test statistics of genes with valid null hypothesis are t-distributed with additional degrees of freedom compared to the unmoderated t-test.[7,8] Multiple testing correction was done by local false discovery rate estimation using the locfdr-tool following transformation of our t-scores to z-scores. The locfdr-tool uses a mixture distribution approach with parametric empirical null estimation in order to calculate the local false discovery rates.[9] Gene lists were generated for up to 300 top genes with smallest p-values in pairweise group comparisons.

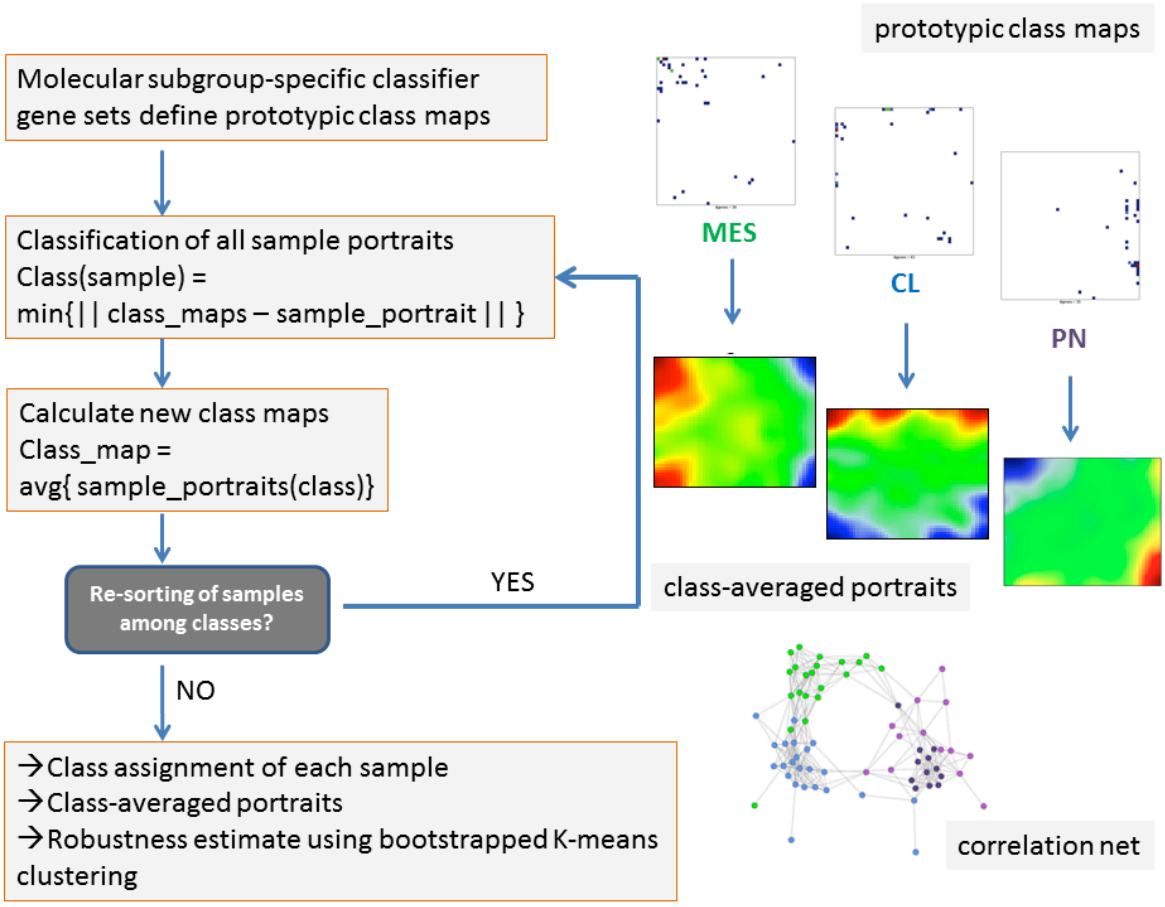

Supplementary Figure 2. Strategy used for the classification of glioblastomas according to molecular subgroups (mesenchymal, classical, proneural).[6] The prototypic class maps show the classifier genes of each molecular subgroup considered as dots in SOM space. The class-averaged portraits are mean SOM maps averaged over all individual maps showing closest similarity with the respective prototypic map. Red overexpression spots in the class-averaged portraits tend to appear in regions accumulating the respective classifier genes. The correlation net shows disjunct subgroup-specific clusters after running the algorithm (see Supplementary Figure 3).

Analysis of array-CGH data

Of the 89 glioblastoma samples that were analysed by array-CGH, three cases were excluded from the analysis because of poor hybridisation quality. Our microarrays contained 3,000 bacterial artificial chromosome clones from the Sanger Centre 1 Mb clone set,[10] 3,000 additional gene- and region-specific bacterial artificial chromosome clones of the Roswell Park Cancer Institute (RZPD, Berlin, Germany) and California Institute of Technology (Invitrogen, Karlsruhe, Germany) collections,[11] 2,000 clones providing tiling-path resolution of the large GC- and gene-rich regions on chromosomes 1, 19 and 22, and 2,000 clones providing high resolution of selected disease/tumor-relevant chromosomal regions. Microarrays were hybridised with Cy3-labeled tumor DNA and Cy5-labeled reference DNA. Pooled reference DNA samples were from 10 healthy individuals and gender-matched. For quality evaluation, the whole array-CGH profile of each case was considered. As the first pre-processing step for each microarray, we performed a normalisation by using a robust mode estimator. This was followed by circular binary segmentation (CBS) using a permutation-based test with a significance level of 0.01 to determine the breakpoints. Segmentation also allowed for the calculation of a robust noise estimator, which was the median absolute deviation (MAD) of the normalised values from the segments median, i.e. the segment value given in units of log2 of the copy number. This robust noise estimator was used to calculate a microarray-specific threshold to classify genomic imbalances: Segment values with an absolute value higher than 1.3xMAD were considered as gains, segment values with an absolute value lower than -1.3xMAD were considered as losses.[12]

Supplementary results

SOM expression portraits and characterization of molecular subclasses as well as expression modules

SOM portraying revealed a variety of different expression patterns that could be assigned to molecular subtypes of glioblastomas as proposed by Verhaak et al.,[6] i.e. mesenchymal, classical and proneural subtypes. Each subclass is characterized by a unique mean SOM landscape, with partial overlap between the mesenchymal and classical tumor groups on one hand and the two proneural subgroups, i.e. *IDH1/2*-mutant and *IDH1/2*-wildtype tumors, on the other (Supplementary Figure 3). Robustness of classification is above 90% for most of the samples except for samples in the overlap regions (robustness 50 – 80%). Addition of the neuronal subtype reported by Verhaak et al.[6] as fourth class did not change the results, i.e., no sample was assigned to this subtype. Thus, tumors corresponding to the neuronal subtype were missing in our cohort. A very heterogeneous distribution of classifier genes for the neuronal subtype in the SOM portrait supported this hypothesis (data not shown).

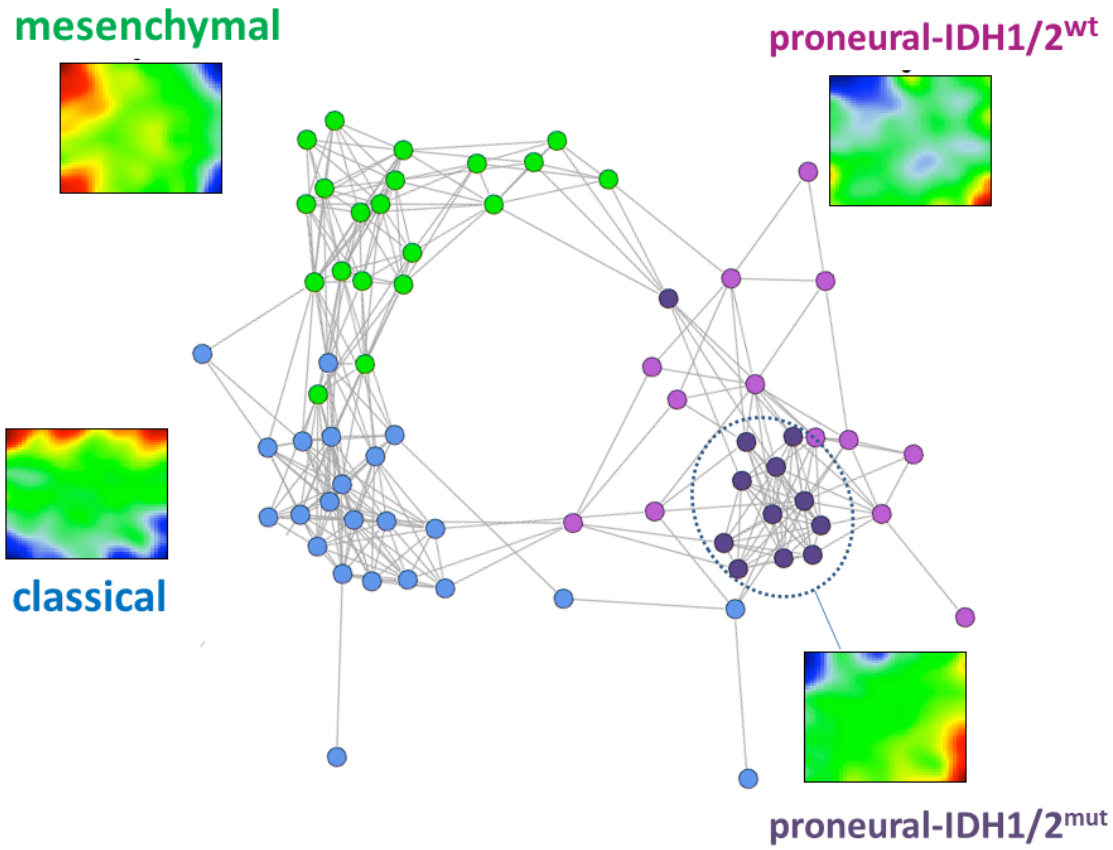

Supplementary Figure 3. Correlation net representation after classification of the tumors into classical, mesenchymal and proneural subtypes. The mean SOM portraits reflect the average expression landscapes over all cases of each individual tumor subtype. This correlation net illustrates the relation between the molecular subtypes with the samples assigned to the mesenchymal and classical tumors forming a continuum disjunct from the proneural tumors. Note also the systematic differences of the mean SOM portraits specifying characteristic expression differences and similarities between the molecular subgroups. For example, the mesenchymal and classical subtypes possess a set of commonly up- or down-regulated genes located in the left upper and right lower corners of the map, which show antagonistic expression behavior in both proneural subtypes. Genes differentiating between the mesenchymal and proneural subtypes are mostly located along the upper, lower and left borders of the map.

Analyses for differential gene expression in the distinct survival groups

To characterize expression differences between the three patient cohorts with distinct overall survival, we applied SOM-based differential mapping and standard differential analyses using t-test statistics. The SOM difference maps revealed clear expression differences between long-term (group A) and short-term survivors (group B), as well as between *IDH1/2*^{mut} and *IDH1/2*^{wt} glioblastomas. However, virtually no differences between the different survival groups of patients with *IDH1/2*^{wt} glioblastomas were detected after multitest adjustment (Supplementary Figure 4). Lists of up to 300 top differentially expressed genes obtained by standard two-group comparative analyses were generated for group A versus group B, group *IDH1/2*^{wt} versus group *IDH1/2*^{mut}, and group A^{wt} versus group B^{wt}; respectively. We mapped the three lists into SOM space and generated boxplots of the mean expression per list to compare the expression levels between the different subgroups (Supplementary Figure 4). Thereby, we detected genes in localized regions of the map that agreed with the spots already detected in the SOM portrays of the tumor samples (for comparison see Supplementary Supplementary Figure **4**). Other genes were distributed randomly over the map with low local density. These latter genes are likely to be false positive candidates while the localised genes are of potential interest. In Supplementary Table 3 we provide the genes located in the highly populated spot regions of each of the lists for up- or down-regulated genes in the respective pair comparisons.

Interestingly, the genes found to be differentially expressed between tumors from group A and group B essentially accumulated in the same regions as the genes found to be differentially expressed between *IDH1/2*^{mut} and *IDH1/2*^{wt} glioblastomas, respectively. This finding suggests that most of the differential gene expression between group A and group B patients is due to the differential distribution of *IDH1/2*^{mut} versus *IDH1/2*^{wt} tumors in these groups. Note that the two gene lists of the top 300 differentially expressed genes overlap only in six genes (*TOM1L1, TGIF1, E2F7, RAB36, PCDH21, S100A11*) whereas the spot-related selection criteria provided more than two hundred up- or down-regulated genes showing concerted expression profiles in the sample set studied. Application of this criterium of mutual co-regulation of the genes from the spots obviously selects longer lists and removes false positives, thus enabling the detection of genes of associated functional impact in different groups of samples with increased resolution.

The comparison of *IDH1/2*^{wt} glioblastomas from long-term (group A^{wt}) and short-term survivors (group B^{wt}) revealed only two faint differentially expressed spots (grey arrows in the log p-value map in Supplementary Figure 4). However, these were localized in spot areas typical for mesenchymal and classical glioblastomas, and thus might reflect subtle differences in the expression patterns of glioblastomas of both subtypes present in group A^{wt} and group B^{wt}, respectively. Moreover, these differences lacked significance after multitest adjustment. Hence, we concluded that group A^{wt} and group B^{wt} tumors show no differential gene expression (fdr map in Supplementary Figure 4). In contrast, the *IDH1/2*^{mut} tumors from long-term survivors demonstrated a clearly different expression profile as compare to *IDH1/2*^{wt} tumors from any of the three survival groups (see red spots in the respective fdr-map in Supplementary Supplementary Figure **4**).

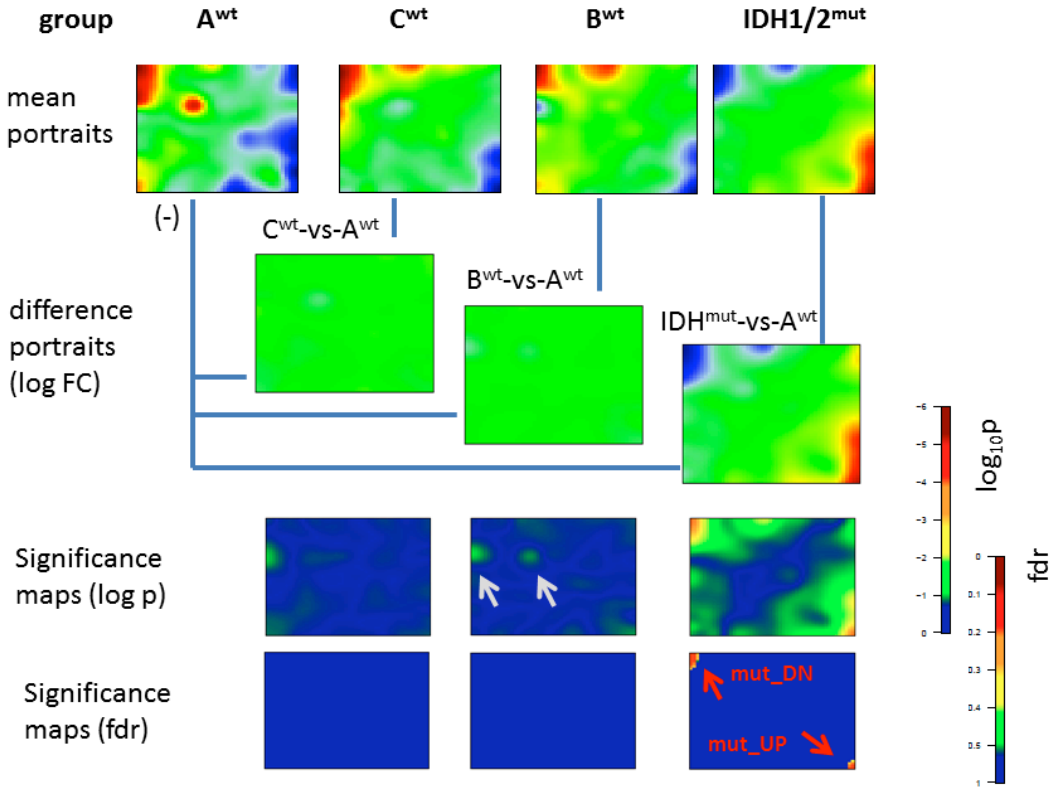

Supplementary Figure 4. Group-specific mean portraits, difference SOM portraits with respect to the *IDH1/2*-wildtype glioblastomas from long-term survivors (group A^{wt}), as well as log p- and fdr (local false discovery rate)-significance maps (respective color scales are indicated on the right side of the maps). The mean SOM portraits differ clearly between *IDH1/2*-mutant glioblastomas from long-term survivors and *IDH1/2*-wildtype glioblastomas from each of the three survival groups (groups A^{wt}, B^{wt} and C^{wt}), which are very similar. The difference portraits support this observation, i.e., there are almost no expression differences in the comparisons of group A^{wt} with group B^{wt} or group C^{wt}, respectively (all three maps are colored in identical scale). In log p scale, the green spots provide log p<-1 in group A^{wt} versus group B^{wt} comparison (light-grey arrows), which, however, lacked significance after multitest adjustment. In contrast, differential expression of genes in the top-left and bottom-right corners remained significant in the comparison of *IDH1/2*-wildtype (group A^{wt}) with *IDH1/2*-mutant (group A^{mut}) glioblastomas from long-term survivors (fdr<0.1, see red arrows in the significance maps). Note that the respective spots refer to genes down- or up-regulated in *IDH1/2*-mutant tumors compared with *IDH1/2*-wildtype tumors as indicated in the figure (mut_DN and mut_UP, respectively).

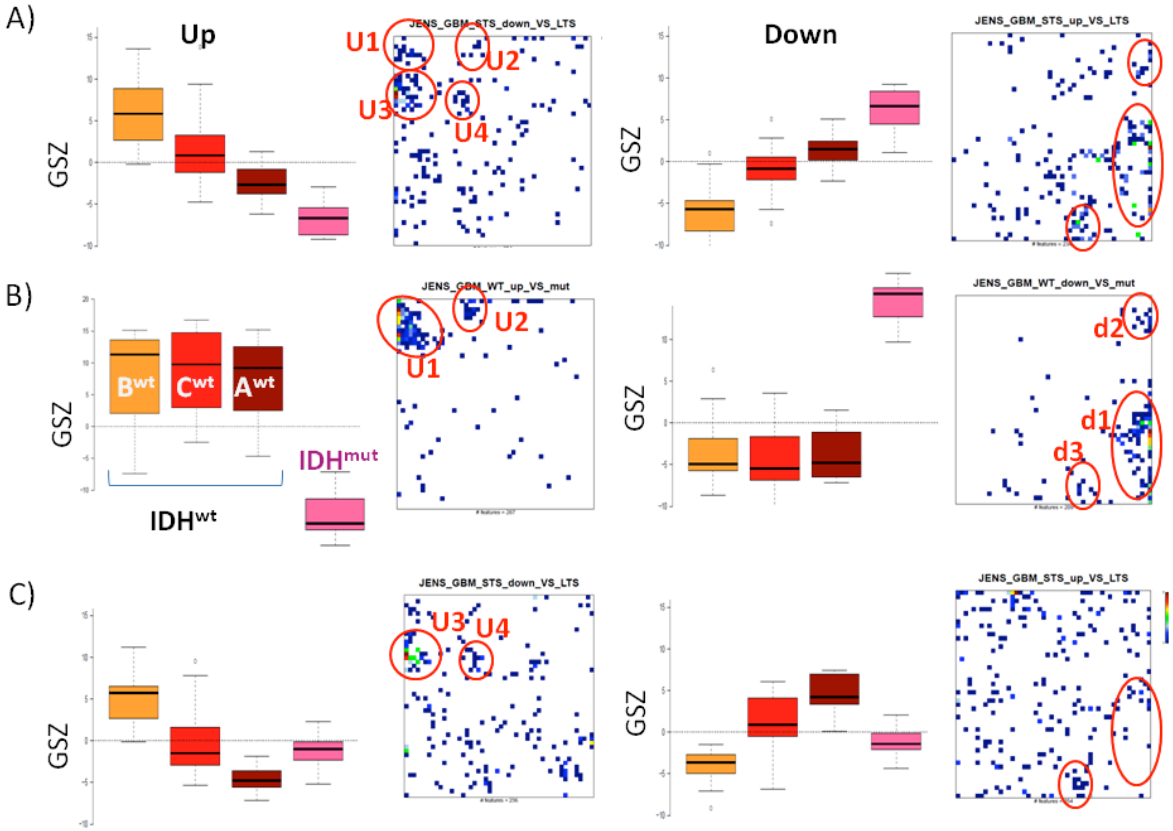

Supplementary Figure 5. Mean GSZ-profiles and gene set population maps obtained by two-group comparisons of **(A)** glioblastomas from short-term versus long-term survivors (group B versus group A); **(B)** *IDH1/2*-wildtype versus *IDH1/2*-mutant tumors (group *IDH1/2*^{wt} versus *IDH1/2*^{mut}), and **(C)** *IDH1/2*-wildtype glioblastomas from short-term versus long-term survivors (group B^{wt} versus group A^{wt}). Boxplots of the mean GSZ-expression levels and gene sets population maps of up-regulated or of down-regulated genes are separately shown in the left and right part of the figure, respectively. The boxplots show the expression levels of the three *IDH1/2*-wildtype survival groups (A^{wt}, B^{wt} and C^{wt}) and of the *IDH1/2*-mutant group (*IDH1/2*^{mut}) in units of the GSZ score as assigned in panel B. The population maps project the positions of the genes considered in each of the lists into SOM space. The red circles label regions of enriched local densities of genes. Note that two-group comparisons of *IDH1/2*^{wt} versus *IDH1/2*^{mut} (panel B), and group B^{wt} versus group A^{wt} (panel C) select up-regulated genes that accumulate in different areas of the SOM (U1 and U2 versus U3 and U4, respectively). In contrast, genes extracted from the group B versus group A comparison (panel A) accumulate in regions U1 and U2 as well as U3 and U4 because particularly group A contains both *IDH1/2*-mutant and *IDH1/2*-wildtype tumors.

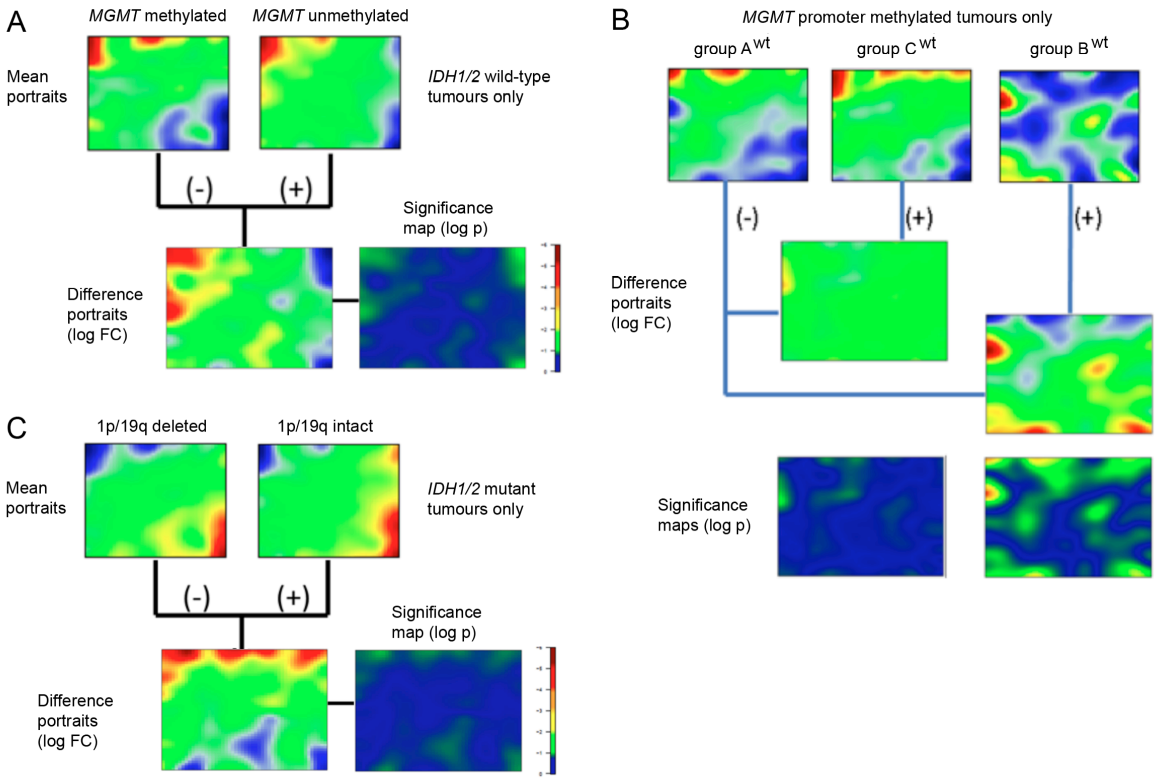

Supplementary Figure 6. Differential expression analyses in SOM space showing mean SOM portraits of selected tumor groups, their difference portraits and and significance maps. (**A)** *IDH1/2*^{wt} tumors with methylated *MGMT* promoter compared to *IDH1/2*^{wt} tumors with unmethylated *MGMT* promoter. **(B)** *IDH1/2*^{wt} tumors with methylated *MGMT* promoter stratified into survival groups A^{wt}, B^{wt}, and C^{wt}, respectively. **(C)** *IDH1/2*^{mut} tumors stratified according to the 1p/19q deletion status. The individual groups show difference portraits with distinctive spot patterns. However, these generally refer to fdr values greater than 0.5 after multitest adjustment and thus do not support significant differential gene expression.

Supplementary results obtained by array-CGH analysis and combination of array-CGH and mRNA expression data

Supplementary Figures 7 and 8 provide additional information about the detected array-CGH aberration patterns and associated gene-dosage effects in our tumor cohorts. Supervised clustering of the chromosomal aberrations according to the molecular subtypes of glioblastoma confirmed that *IDH1/2* wildtype tumors show frequent gain of chromosome 7 and loss of chromosome 10. Most of the classical and mesenchymal tumor additionally demonstrated gains on chromosomes 19 and 20, as well as losses on chromosome 22. A few samples of the classical, mesenchymal and proneural *IDH1/2*^{wt} type subclasses show complex genomic imbalances affecting multiple chromosomes. Deletions of 1p and 19q were detected in a subset of *IDH1/2*^{mut} proneural tumors.

Significant differences in gene dosage effects on mRNA expression of genes located in gained or lost regions of each of the chromosomes were observed nearly exclusively when comparing the group of *IDH1/2*^{mut} tumors with the *IDH1/2*^{wt} groups (A^{wt}, B^{wt} and C^{wt}). Losses on chromosome 14 were more common in group A^{wt} than in group C^{wt} tumors, however, had only week effects on differential gene expression in this group.

Separate gene dosage analyses for the short and long arm of each chromosome in most instancies provided similar results as obtained for entire chromosomes, including chromosomes 7 and 10 (not shown). In contrast, in case of chromosomes 1 and 19, the gene dosage effects of losses were restricted to genes on the p- and q-arms, respectively.

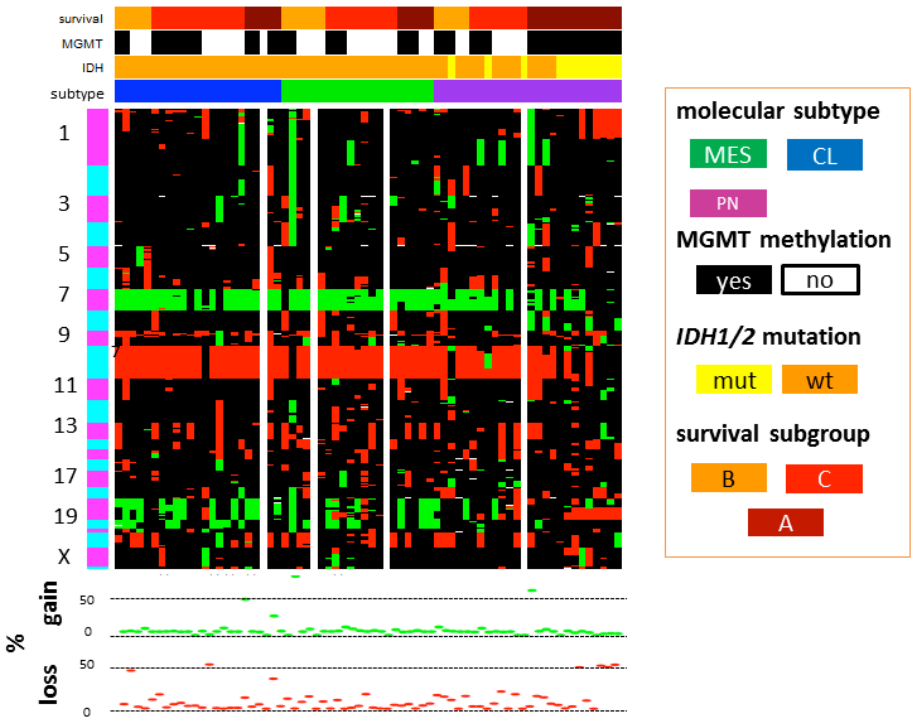

Supplementary Figure 7. Results of supervised clustering of chromosomal imbalances detected by array-CGH according to transcriptome-based molecular subtypes of glioblastoma (classical, mesenchymal, proneural). The distinct survival groups, *IDH1/2* mutation status, and *MGMT* promoter methylation status are also indicated on top of the figure. The graph below the heatmap indicates the total fraction of chromosomal segments demonstrating copy number gains or losses in each tumor sample.

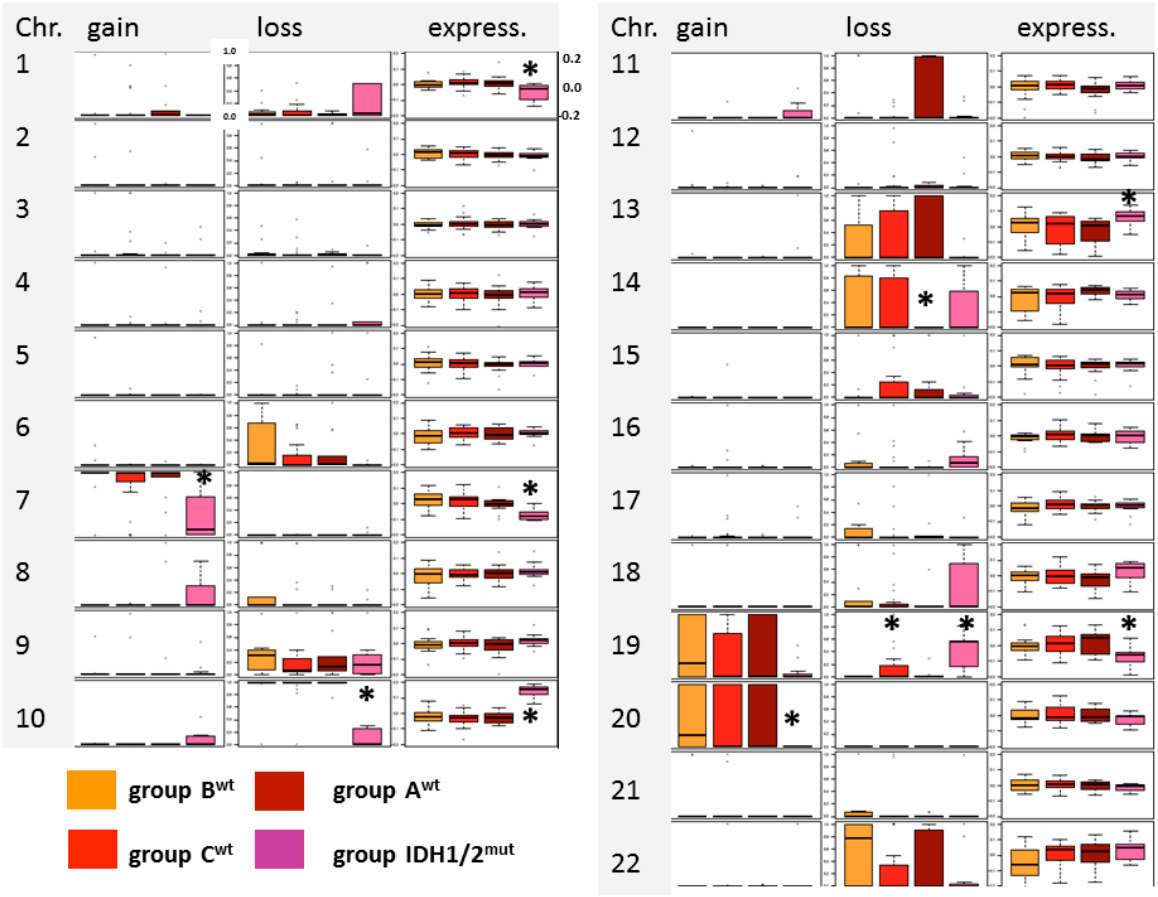

Supplementary Figure 8. Results of combined analysis of mRNA expression data and array-CGH data illustrating gene dosage effects of certain chromosomal imbalances. The boxplots indicate the percentage of gains or losses involving each chromosome and the relative expression values of all genes located on the respective chromosomes in the distinct patients groups. Significant differences are indicated by stars. Gene dosage effects are detectable for several copy number changes including among others gains of chromosome 7 and losses of chromosomes 10 and 19. However, differences are mostly evident between the three groups of *IDH1/2*-wildtype tumors on the one hand and the *IDH1/2*-mutant tumors on the other hand. Among the *IDH1/2*-wildtype tumor groups, loss of chromosome 14 was less frequent in group C^{wt} tumors while losses of chromosome 19 was more frequent in group B^{wt} tumors, respectively. However, both changes did not associate with significant differential gene dosage effects. Please note the scales: For chromosome 7 the boxplots indicate close to 100% gains and likewise on chromosome 10 almost 100% loss in groups A^{wt}, B^{wt}, C^{wt} (ceiling effect).

Comparative analysis of published prognostic gene signatures in the own expression data set

We also used the SOM space based on our own data to analyse the prognostic significance of various published prognostic gene signatures in our cohort of glioblastoma patients. Supplementary Figure 4 shows gene set population maps for the individual gene signatures reported by different authors. These plots highlight that the various signatures weakly differ between each other. Most pick up mesenchymal and classical signature genes that are up-regulated in the respective glioblastoma subtypes but down-regulated in proneural tumors (compare also with the maps shown in Supplementary Figures 4 and 5). The signatures reported by Colman et al.,[13] Philips et al.,[14] Kim et al.,[15] and Nutt et al.[16] primarily discriminate between *IDH1/2*^{mut} and *IDH1/2*^{wt} tumors of our series. Donson et al.[17] and Barbus et al.[18] reported on signatures that are more related to *IDH1/2*^{wt} tumors, for which we cannot detect a survival difference in our patients. Again, the signature genes of Donson et al.[15] discriminate mainly between proneural (*IDH1/2*^{mut} and *IDH1/2*^{wt}) tumors on the one hand versus mesenchymal and classical tumors on the other hand.

Using the same approach, we also mapped genes reported to be hypermethylated and thus presumably down-regulated in long-term survivors to our SOM portraits (Supplementary Figure 10). These analyses revealed that the differentially methylated genes reported by Noushmehr et al.[19] co-localised with mesenchymal and classical signature genes, i.e., are up-regulated in the respective glioblastoma subtypes relative to the proneural tumor subgoup, which contains the *IDH1/2*^{mut} tumors. Thus, the G-CIMP signature genes primarily discriminate between *IDH1/2*^{mut} and *IDH1/2*^{wt} tumors but not between survival groups of the *IDH1/2*^{wt} glioblastomas. Several of the differentially methylated genes reported by Shinawi et al.[20] similarly distinguish proneural from mesenchymal and classical tumors, respectively. The classifiers reported by Martinez et al.,[21] Christensen et al.[22], and Laffaire et al.[23] do not appear to be very selective in our cohort of patients. However, all four classifiers appear to primarily distinguish between *IDH1/2*^{mut} and *IDH1/2*^{wt} tumors but not between distinct survival groups of patients with *IDH1/2*^{wt} glioblastomas.

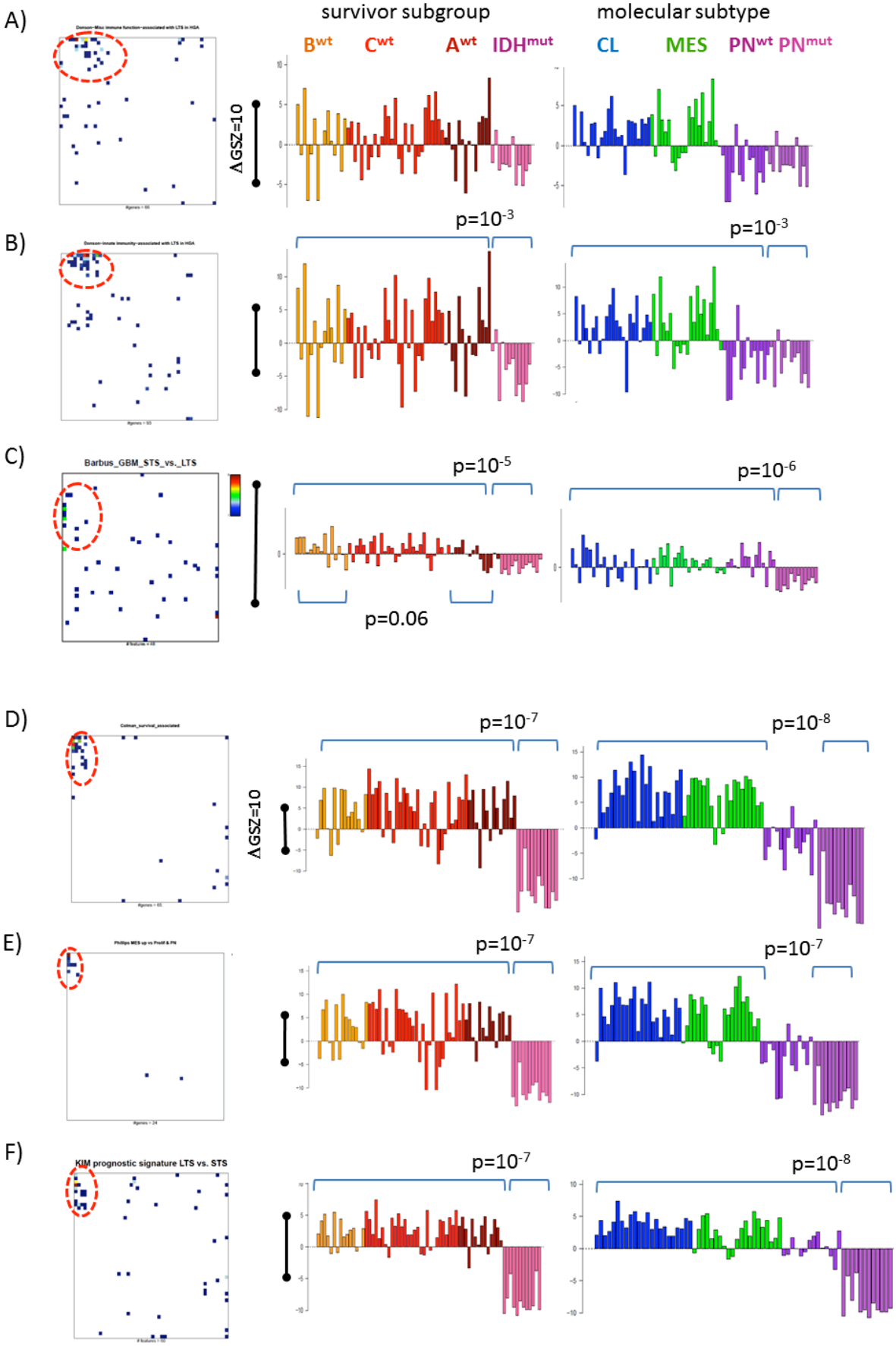
A)
survivor subgroup
molecular subtype
B^wt C^wt A^wt IDH^mut
CL MES PN^wt PN^mut
ΔGSZ=10
B)
p=10^-3
p=10^-3
C)
Barbus_GBM_STS_vs._LTS
p=10^-5
p=10^-6
p=0.06
D)
p=10^-7
p=10^-8
ΔGSZ=10
E)
p=10^-7
p=10^-7
F)
KIM prognostic signature LTS vs. STS
p=10^-7
p=10^-8

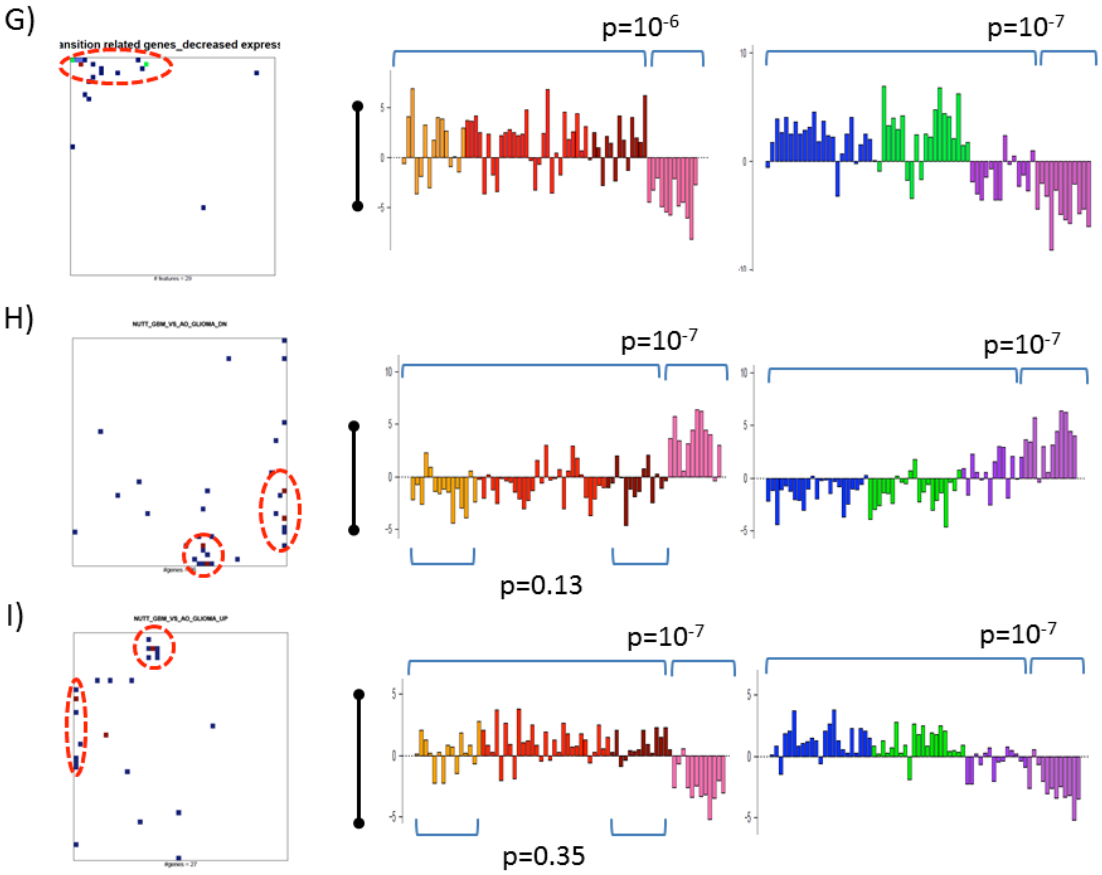

Supplementary Figure 9. Gene set population maps and individual GSZ-profiles of survival-associated genes taken from previous publications addressing prognostic gene expression signatures in malignant glioma and mapped to the SOM portaits based on our present patient cohort. **(A)** 'Immune function' and (**B)** 'innate immunity' signatures of Donson et al.,[17] **(C)** 'survival-associated genes' of Barbus et al.,[18] and **(D)** Colman et al.,[13] **(E)** 'mesenchymal-versus-proneural' gene signature of Philips et al.,[14] **(F)** 'survival-associated genes', and **(G)** 'epithelial-to-mesenchymal transistion-related genes' of Kim et al.,[15] **(H)** 'glioblastoma *versus* anaplastic oligodendroglioma up-regulated', and **(I)** 'glioblastoma *versus* anaplastic oligodendroglioma down-regulated' gene sets of Nutt and coworkers.[16] Highly populated regions are indicated by red circles. Essentially, all gene sets accumulate in the spot regions that differentiate between *IDH1/2*-mutant and *IDH1/2*-wildtype tumors. The bar plots show the mean GSZ-expression level of each gene set for each sample, sorted either according to survival groups or according to molecular subtypes (see panel A for assignment). The expression of the gene sets is given in units of the GSZ-score in which the dumbbell-scale ranges from GSZ=-5 to +5. P-values are given for pairwise group comparisons as indicated by the brackets using the Mann-Whitney U-test.

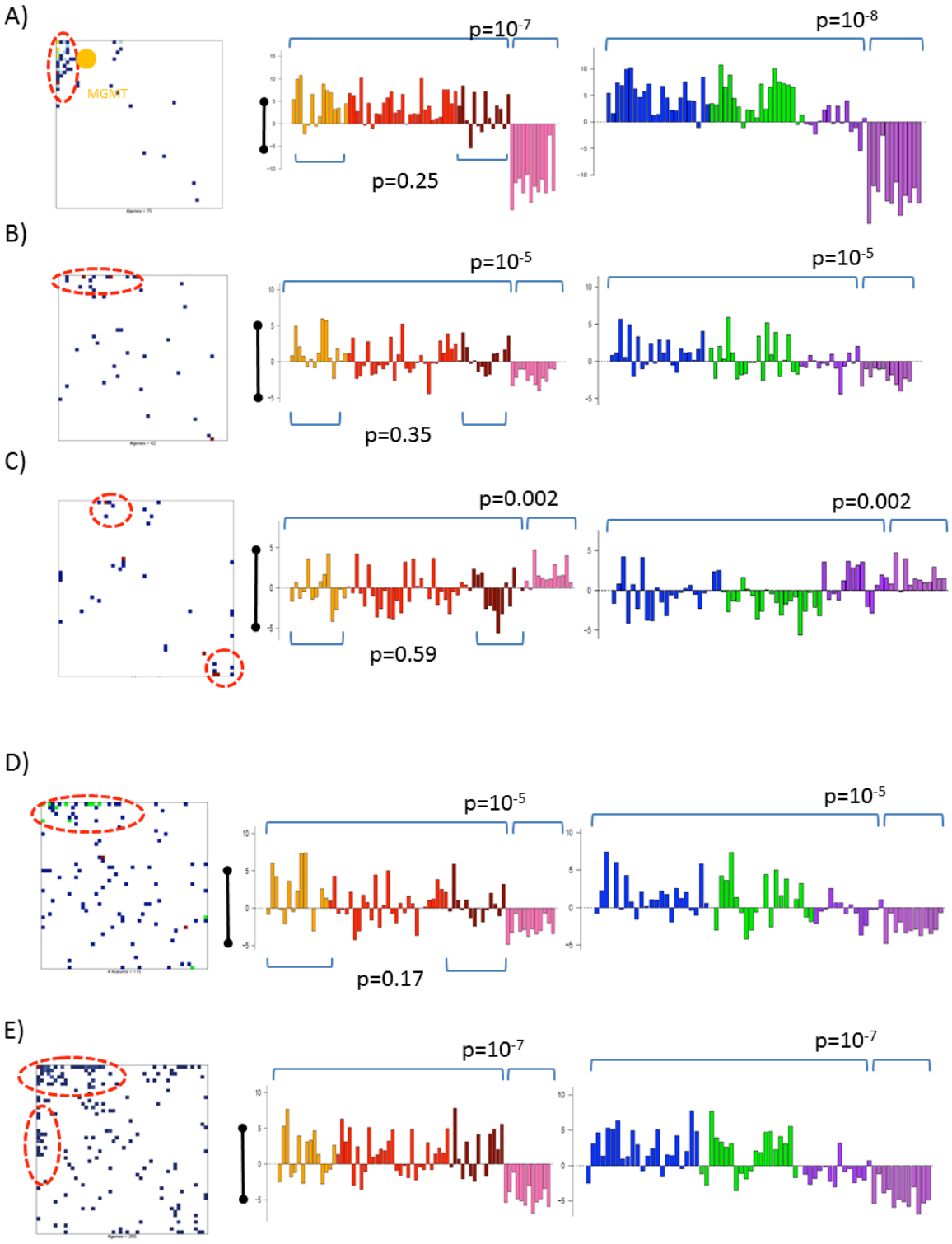

Supplementary Figure 10. Gene set population maps and individual GSZ-profiles of differentially methylated genes were previously linked to *IDH1/2* mutation and/or longer survival in glioblastoma, and were mapped to the SOM maps of our present patient cohort. **(A)** 'G-CIMP methylator phenotype genes' of Noushmehr et al.,[19] **(B)** 'hypermethylated in glioblastoma genes' of Martinez et al.,[21] **(C)** Shinawi et al.,[20] **(D)** Christensen et al.,[22] and **(E)** Laffaire and coworkers.[23] Highly populated regions are indicated by red circles. Essentially all gene sets accumulate in the spot regions that differentiate between *IDH1/2*-mutant and *IDH1/2*-wildtype tumors in our series.

Validation analyses based on TCGA data

We also analysed expression data provided by The Cancer Genome Atlas (TCGA) consortium (https://tcga-data.nci.nih.gov/tcga/) to validate our findings. We started with the core data set of samples most representative for the molecular subtypes determined by Verhaak and coworkers.[6] The respective HT-HG U133A expression raw data were analyzed using our SOM pipeline after hook pre-processing as described in the Methods section above to make the analyses and data sets comparable. Twenty samples did not pass our quality pipeline due to strong batch effects and they were therefore removed from further analysis. To specifically address the question whether *IDH1/2*-wildtype glioblastomas from long-term survivors carry distinct expression profiles when compared to *IDH1/2*-wildtype glioblastomas from short-term or intermediate-term survivors, we selected from the remaining 153 patients those whose tumors were categorized as being *IDH1/2*-wildtype (n=79) and added the subset of tumors that lacked information on the *IDH1/2* mutation status but displayed mesenchymal or classical expression profiles, which are known to associate with the *IDH1/2* wildtype status (n=32) (Supplementary Table 5). The respective HT-HG U133A expression raw data of these 101 tumor samples were analyzed using our SOM pipeline after hook pre-processing as described in the Methods section above. In total, 9 patients with long-term survival of 36 months or more (group $A^{wt\text{-}TCGA}$; median OS: 42.6 months), 48 patients with short-term survival of less than 12 months after diagnosis (group $B^{wt\text{-}TCGA}$; median OS: 6.5 months), 44 patients with intermediate survival (group $C^{wt\text{-}TCGA}$; median OS: 17 months) were investigated.

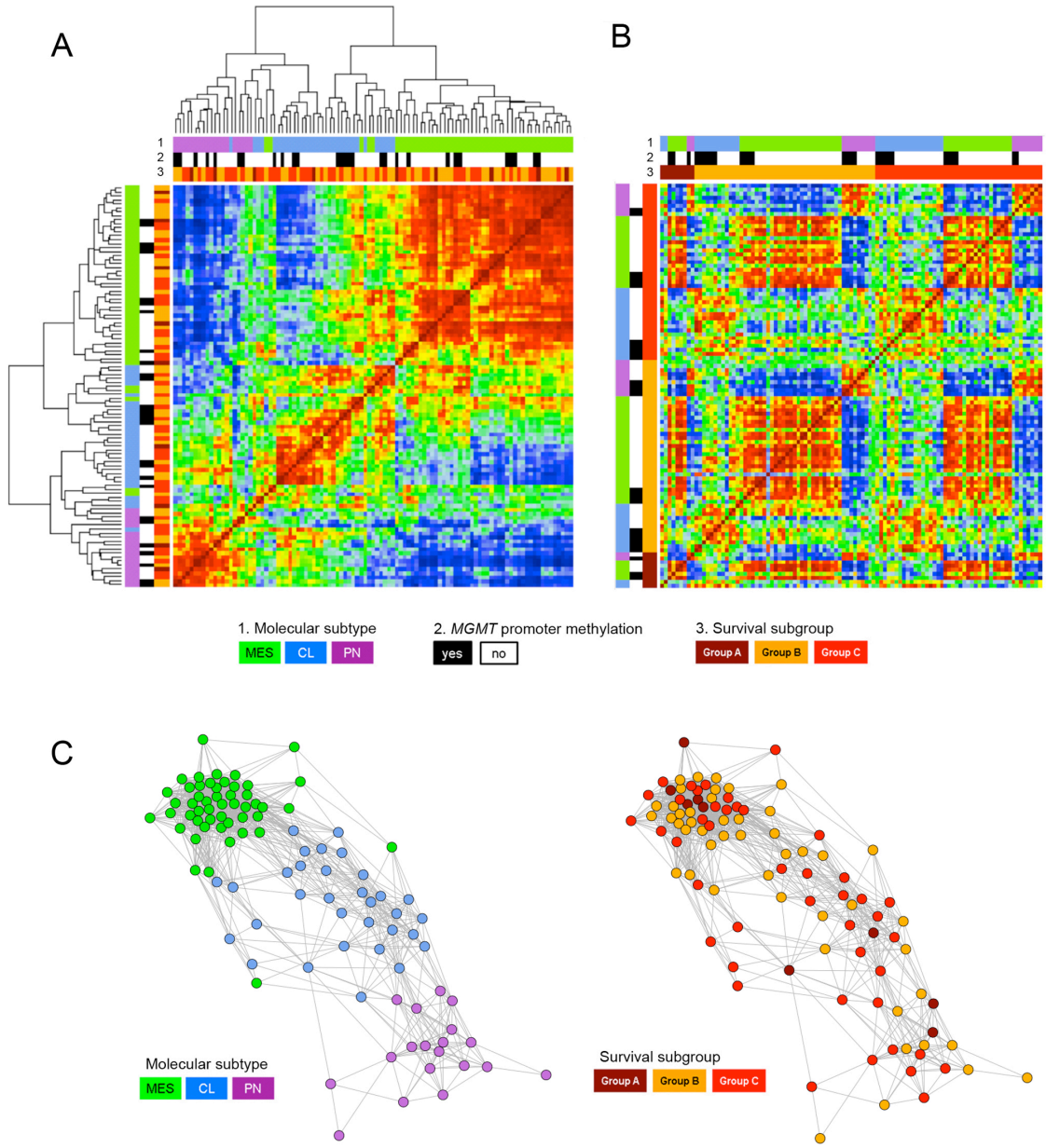

Supplementary Figure 11. Results of a validation analysis using the independent TCGA data set. **(A)** Unsupervised and **(B)** supervised (with respect to the survival groups) pairwise correlation matrix of *IDH1*^{wt} and classical or mesenchymal glioblastomas of the selected TCGA cohort. **(C)** The correlation net colored according to molecular subtypes (left) and survival groups (right). All presentations reveal almost no structure according to patient survival groups. In contrast, the transcriptome-based molecular subtypes reveal clear correlation and anti-correlation patterns, respectively.

Supplementary references

1. Binder H, Preibisch S. "Hook" calibration of GeneChip-microarrays: Theory and algorithm. *Algorithms for Molecular Biology* 2008; **3**: 12.
2. Binder H, Krohn K, Preibisch S. "Hook" calibration of GeneChip-microarrays: chip characteristics and expression measures. *Algorithms for Molecular Biology* 2008; **3**: 11.
3. Wirth H, Löffler M, von Bergen M, Binder H. Expression cartography of human tissues using self organizing maps. *BMC Bioinformatics* 2011; **12**: 306.
4. Wirth H, von Bergen M, Binder H. Mining SOM expression portraits: Feature selection and integrating concepts of molecular function. *BioData Mining* 2012; **5**:18.
5. Strimmer K. A unified approach to false discovery rate estimation. *BMC Bioinformatics* 2008; **9**: 303.
6. Verhaak RG, Hoadley KA, Purdom E, Wang V, Qi Y, Wilkerson MD et al. Integrated genomic analysis identifies clinically relevant subtypes of glioblastoma characterized by abnormalities in PDGFRA, IDH1, EGFR, and NF1. *Cancer Cell* 2010; **17**: 98–110.
7. Loennstedt I, Speed T. Replicated microarray data. *Statistica Sinica* 2002; **12**: 41-6.
8. Smyth GK. Linear models and empirical bayes methods for assessing differential expression in microarray experiments. *Stat Appl Genet Mol Biol* 2004; **3**: Article 3.
9. Efron B, Tibshirani R. On testing the significance of sets of genes. *Ann Appl Stat* 2007; **1**: 107-29.
10. Fiegler H, Carr P, Douglas EJ, Burford DC, Hunt S, Scott CE et al (2003) DNA microarrays for comparative genomic hybridization based on DOP-PCR amplification of BAC and PAC clones. Genes Chromosomes Cancer 36: 361-74.
11. Zielinski B, Gratias S, Toedt G, Mendrzyk F, Stange DE, Radlwimmer B et al. Detection of chromosomal imbalances in retinoblastoma by matrix-based comparative genomic hybridization. *Genes Chromosomes Cancer* 2005; **43**: 294–301.
12. Kreuz M, Rosolowski M, Berger H, Schwaenen C, Wessendorf S, Loeffler M et al. Development and implementation of an analysis tool for array-based comparative genomic hybridization. *Methods Inf Med* 2007; **46**: 608–13.
13. Colman H, Zhang L, Sulman EP, McDonald JM, Shooshtari NL, Rivera A et al. A multigene predictor of outcome in glioblastoma. *Neuro-Oncol* 2010; **12**: 49-57.
14. Phillips HS, Kharbanda S, Chen R, Forrest WF, Soriano RH, Wu TD et al. Molecular subclasses of high-grade glioma predict prognosis, delineate a pattern of disease progression, and resemble stages in neurogenesis. *Cancer Cell* 2006; **9**: 157-73.
15. Kim YW, Koul D, Kim SH, Lucio-Eterovic AK, Freire PR, Yao J et al. Identification of prognostic gene signatures of glioblastoma: a study based on TCGA data analysis. *Neuro-Oncol* 2013; **15**: 829-39.
16. Nutt CL, Mani DR, Betensky RA, Tamayo P, Cairncross JG, Ladd C et al. Gene expression-based classification of malignant gliomas correlates better with survival than histological classification. *Cancer Res* 2003; **63**: 1602–7.
17. Donson AM, Birks DK, Schittone SA, Kleinschmidt-DeMasters BK, Sun DY, Hemenway MF et al. Increased immune gene expression and immune cell infiltration in high-grade astrocytoma distinguish long-term from short-term survivors. *J Immunol* 2012; **189**: 1920–7.
18. Barbus S, Tews B, Karra D, Hahn M, Radlwimmer B, Delhomme N et al. Differential retinoic acid signaling in tumors of long- and short-term glioblastoma survivors. *J Natl Cancer Inst* 2011; **103**: 598–606.
19. Noushmehr H, Weisenberger DJ, Diefes K, Phillips HS, Pujara K, Berman BP et al. Identification

of a CpG island methylator phenotype that defines a distinct subgroup of glioma. *Cancer Cell* 2010; **17**: 510–22.

20. Shinawi T, Hill VK, Krex D, Schackert G, Gentle D, Morris MR et al. DNA methylation profiles of long- and short-term glioblastoma survivors. *Epigenetics* 2013; **8**: 149-56.
21. Martinez R, Martin-Subero JI, Rohde V, Kirsch M, Alaminos M, Fernandez AF et al. A microarray-based DNA methylation study of glioblastoma multiforme. *Epigenetics* 2009; **4**: 255-64.
22. Christensen BC, Smith AA, Zheng S, Koestler DC, Houseman EA, Marsit CJ et al. DNA methylation, isocitrate dehydrogenase mutation, and survival in glioma. *J Nat Cancer Inst* 2011; **103**: 143-53.
23. Laffaire J, Everhard S, Idbaih A, Crinière E, Marie Y, de Reyniès A et al. Methylation profiling identifies 2 groups of gliomas according to their tumorigenesis. *Neuro-Oncol* 2011; **13**: 84-98.

Supplementary tables

Supplementary Table 1. Summary of clinical, histological, and molecular characteristics for all 94 patients according to survival groups.

	Total n=94	Group A n=28	Group B n=20	Group C n=46
Age at diagnosis (years)				
Median (range)	58 (25-80)	52 (25-74)	63 (37-80)	59 (28-74)
Age classes				
< 51	29 (30.9%)	14 (50.0%)	3 (15.0%)	12 (26.1%)
51-60	23 (24.5%)	6 (21.4%)	5 (25.0%)	12 (26.1%)
61-70	36 (38.3%)	6 (21.4%)	9 (45.0%)	21 (45.7%)
>70	6 (6.4%)	2 (7.1%)	3 (15.0%)	1 (2.2%)
Gender				
Female	34 (36.2%)	14 (50.0%)	8 (40.0%)	12 (26.1%)
Male	60 (63.8%)	14 (50.0%)	12 (60.0%)	34 (73.9%)
KPS				
<70	5 (5.3%)	1 (3.6%)	2 (10.0%)	2 (4.3%)
70-80	45 (47.9%)	17 (60.7%)	9 (45.0%)	19 (41.3%)
90-100	44 (46.8%)	10 (35.7%)	9 (45.0%)	25 (54.3%)
Surgery				
Total	47 (50.0%)	12 (42.9%)	8 (40.0%)	27 (58.7%)
Subtotal	27 (28.7%)	8 (28.6%)	8 (40.0%)	11 (23.9%)
Partial	12 (12.8%)	3 (10.7%)	4 (20.0%)	5 (10.9%)
Biopsy	2 (2.1%)	1 (3.6%)	-	1 (2.2%)
Unknown	6 (6.4%)	4 (14.3%)	-	2 (4.3%)
Review diagnosis				
Glioblastoma	84 (89.4%)	22 (78.6%)	19 (95.0%)	43 (93.5%)
Giant cell glioblastoma	1 (1.1%)	-	-	1 (2.2%)
Gliosarcoma	3 (3.2%)	1 (3.6%)	1 (5.0%)	1 (2.2%)
Glioblastoma with oligodendroglial component	6 (6.4%)	5 (17.9 %)	-	1 (2.2 %)

***MGMT* promoter methylation status**				
Methylated	41 (43.6%)	21 (75.0%)	5 (25.0%)	15 (32.6%)
Weakly methylated	9 (9.6%)	4 (14.3%)	2 (10.0%)	3 (6.5%)
Unmethylated	44 (46.8%)	3 (10.7%)	13 (65.0%)	28 (60.9%)
***IDH1/2* mutation status**				
IDH1-mutant	14 (14.9%)	10 (35.7%)	1 (5.0%)	3 (6.5%)
IDH2-mutant	1 (1.1%)	1 (3.6%)	-	-
IDH1/2-wildtype	79 (84.9%)	17 (60.7%)	19 (95.0%)	43 (93.5%)
First-line therapy				
No therapy	1 (1.1%)	1 (3.6%)	-	-
RT	8 (8.5%)	3 (10.7%)	-	5 (10.9%)
RT plus TMZ	84 (89.4%)	24 (85.7%)	20 (100%)	40 (87.0%)
TMZ	1 (1.1%)	-	-	1 (2.2%)
Median PFS (95%-CI) in months (events)	6.4 (2.7 – 10.1) (89/94)	26.2 (24.4 - 28.0) (23/28)	3.5 (2.8 – 4.3) (20/20)	6.1 (5.4 – 6.8) (46/46)
First salvage therapy				
Surgery alone	15 (16.0%)	3 (10.7%)	1 (5.0%)	11 (23.9%)
Surgery plus CT	32 (34.0%)	8 (28.6%)	3 (15.0%)	21 (45.7%)
RT plus CT	5 (5.3%)	3 (10.7%)	-	2 (4.3%)
CT alone	13 (13.8%)	5 (17.9%)	1 (5.0%)	7 (15.2%)
OP plus other	1 (1.1%)	-	-	1 (2.2%)
No therapy	28 (29.8%)	9 (32.1%)	15 (75.0%)	4 (8.7%)
Lines of salvage therapy				
1	12 (12.8%)	5 (17.9%)	1 (5.0%)	6 (13.0%)
2	4 (4.3%)	2 (7.1%)	-	2 (4.3%)
>2	3 (3.2%)	2 (7.1%)	-	1 (2.2%)
Median OS (95%-CI) in months (events)	18.7 (16.6-22.7) (85/97)	50.4 (42.0-58.8) (19/28)	4.6 (4.1-5.1) (20/20)	16.7 (14.6-18.8) (46/46)

Supplementary Table 2. Summary of clinical, histological, and molecular characteristics for the group of 79 patients with *IDH1/2*-wildtype glioblastomas according to survival groups.

	Total^{wt} n=79	**Group A^{wt} n=17**	**Group B^{wt} n=19**	**Group C^{wt} n=43**
Age at diagnosis (years)				
Median (range)	61 (25-80)	59 (25-74)	64 (37-80)	61 (38-74)
Age classes				
< 51	16 (20.3%)	4 (23.5%)	2 (10.5%)	10 (23.3%)
51-60	22 (27.8%)	6 (35.3%)	5 (26.3%)	11 (25.6%)
61-70	35 (44.3%)	5 (29.4%)	9 (47.4%)	21 (48.8%)
>70	6 (7.6%)	2 (11.8%)	3 (15.8%)	1 (2.3%)
Gender				
Female	30 (38.0%)	10 (58.8%)	8 (42.1%)	12 (27.9%)
Male	49 (62.0%)	7 (41.2%)	11 (57.9%)	31 (72.1%)
KPS				
<70	4 (5.1%)	-	2 (10.5%)	2 (4.7%)
70-80	38 (48.1%)	12 (70.6%)	8 (42.1%)	18 (41.9%)
90-100	37 (46.8%)	5 (29.4%)	9 (47.4%)	23 (53.5%)
Surgery				
Total	41 (51.9%)	8 (47.1%)	7 (36.8%)	26 (60.5%)
Subtotal	25 (31.6%)	6 (35.3%)	8 (42.1%)	11 (25.6%)
Partial	8 (10.1%)	1 (5.9%)	4 (21.1%)	3 (7.0%)
Biopsy	2 (2.5%)	1 (5.9%)	-	1 (2.3%)
Unknown	3 (3.8%)	1 (5.9%)	-	2 (4.7%)
Review diagnosis				
Glioblastoma	74 (93.7%)	15 (88.2%)	18 (94.7%)	41 (95.3%)
Giant cell glioblastoma	1 (1.3%)	-	-	1 (2.3%)
Gliosarcoma	3 (3.8%)	1 (5.9%)	1 (5.3%)	1 (2.3%)
Glioblastoma with oligodendroglial component	1 (1.3%)	1 (5.9%)	-	-
***MGMT* promoter methylation status**				
Methylated	31 (39.2%)	12 (70.6%)	5 (26.3%)	14 (32.6%)

Weakly methylated	5 (6.3%)	2 (11.8%)	1 (5.3%)	2 (4.7%)
Unmethylated	43 (54.4%)	3 (17.6%)	13 (68.4%)	27 (62.8%)
First-line therapy				
No therapy	-	-	-	-
RT	4 (5.1%)	-	-	4 (9.3%)
RT plus CT	75 (94.9%)	17 (100%)	19 (100%)	39 (90.7%)
CT	-	-	-	-
Median PFS (95%-CI) in months (events)	5.8 (4.7-6.9) (78/79)	24.0 (20.4-27.7) (16/17)	3.8 (3.1-4.4) (19/19)	6.1 (5.3-6.9) (43/43)
First salvage therapy				
Surgery alone	12 (15.2%)	-	1 (5.3%)	11 (25.6%)
Surgery plus CT	29 (36.7%)	6 (35.3%)	3 (15.8%)	20 (46.5%)
RT plus CT	4 (5.1%)	3 (17.6%)	-	1 (2.3%)
CT alone	11 (13.9%)	4 (23.5%)	1 (5.3%)	6 (14.0%)
OP plus other	1 (1.3%)	-	-	1 (2.3%)
No therapy	22 (27.8%)	4 (23.5%)	14 (73.7%)	4 (9.3%)
Lines of salvage therapy				
1	10 (12.7%)	4 (23.5%)	1 (5.3%)	5 (11.6%)
2	3 (3.8%)	1 (5.9%)	-	2 (4.7%)
>2	2 (2.5%)	1 (5.9%)	-	1 (2.3%)
Median OS (95%-CI) in months (events)	17.0 (13.6-20.3) (74/79)	45.0 (37.3-52.6) (19/19)	4.7 (4.3-5.1) (12/17)	17.9 (14.5-21.3) (43/43)

Supplementary Table 3. List of genes showing differential expression between glioblastomas from short-term survivors (group B) versus long-term survivors (group A). The genes were selected from the top-ranked 300 genes with smallest p-values that in addition met the condition of spot-membership in one of the regions of increased local population density (see **Supplementary Figure 5**). Lists are given separately for up- and down-regulated genes in group B. The column 'spot membership' assigns the respective spot.

List of 91 genes significantly upregulated in tumors of group B patients (short-term survivors) versus tumors of group A patients (long-term survivors):

Affymetrix Probeset ID	Gene symbol	Gene description	Expression fold change	p-value	Local FDR	Spot membership
229146_at	C7orf31	chromosome 7 open reading frame 31	1.53	0.0001	1	U3
231018_at	LOC342979	hypothetical LOC342979	1.46	0.0002	1	U3
240261_at	TOM1L1	target of myb1 (chicken)-like 1	1.46	0.0003	1	U3
229782_at	RMST	rhabdomyosarcoma 2 associated transcript (non-coding RNA)	1.82	0.0008	1	U3
236255_at	KIAA1909	KIAA1909 protein	1.42	0.0008	1	U3
229912_at	SDK1	sidekick homolog 1, cell adhesion molecule (chicken)	1.46	0.001	1	U3
219215_s_at	SLC39A4	solute carrier family 39 (zinc transporter), member 4	1.51	0.001	1	U1
243957_at	LOC400464	similar to FLJ43276 protein	1.33	0.002	1	U3
214175_x_at	PDLIM4	PDZ and LIM domain 4	1.79	0.002	1	U1
209368_at	EPHX2	epoxide hydrolase 2, cytoplasmic	1.38	0.002	1	U3
222325_at	RMST	rhabdomyosarcoma 2 associated transcript (non-coding RNA)	1.72	0.002	1	U3
224698_at	FAM62B	family with sequence similarity 62 (C2 domain containing) member B	1.11	0.002	1	U3
204485_s_at	TOM1L1	target of myb1 (chicken)-like 1	1.55	0.002	1	U1
235949_at	TTC26	tetratricopeptide repeat domain 26	1.33	0.002	1	U3
231909_x_at	ODF2L	outer dense fiber of sperm tails 2-like	1.25	0.002	1	U3
220919_s_at	C10orf79	chromosome 10 open reading frame 79	1.18	0.003	1	U3
220144_s_at	ANKRD5	ankyrin repeat domain 5	1.35	0.003	1	U3
237211_x_at	MORN3	MORN repeat containing 3	1.33	0.003	1	U3
222089_s_at	C16orf71	chromosome 16 open reading frame 71	1.20	0.003	1	U3

211564_s_at	PDLIM4	PDZ and LIM domain 4	1.93	0.003	1	U1
244710_at	LRGUK	leucine-rich repeats and guanylate kinase domain containing	1.42	0.003	1	U3
212713_at	MFAP4	microfibrillar-associated protein 4	1.59	0.003	1	U3
222773_s_at	GALNT12	UDP-N-acetyl-alpha-D-galactosamine:polypeptide N-acetylgalactosaminyltransferase 12 (GalNAc-T12)	1.23	0.003	1	U4
220520_s_at	NUP62CL	nucleoporin 62kDa C-terminal like	1.27	0.003	1	U3
211675_s_at	MDFIC	MyoD family inhibitor domain containing	1.36	0.004	1	U3
228415_at			1.19	0.004	1	U3
240968_at			1.19	0.004	1	U3
218691_s_at	PDLIM4	PDZ and LIM domain 4	1.62	0.004	1	U1
233011_at	ANXA1	annexin A1	1.67	0.004	1	U1
228213_at	H2AFJ	H2A histone family, member J	1.24	0.004	1	U3
233999_s_at	TTC26	tetratricopeptide repeat domain 26	1.35	0.005	1	U3
241198_s_at	C11orf70	chromosome 11 open reading frame 70	1.42	0.005	1	U3
220591_s_at	EFHC2	EF-hand domain (C-terminal) containing 2	1.50	0.005	1	U3
229407_at	SDK1	sidekick homolog 1, cell adhesion molecule (chicken)	1.31	0.005	1	U3
243087_at	WDR63	WD repeat domain 63	1.53	0.005	1	U3
229377_at	GRTP1	growth hormone regulated TBC protein 1	1.40	0.005	1	U3
235559_at	FLJ22374	hypothetical protein FLJ22374	1.32	0.005	1	U3
1554528_at	C3orf15	chromosome 3 open reading frame 15	1.40	0.005	1	U3
235144_at			1.63	0.005	1	U3
224699_s_at	FAM62B	family with sequence similarity 62 (C2 domain containing) member B	1.18	0.005	1	U2
223817_at	LRRIQ1	leucine-rich repeats and IQ motif containing 1	1.25	0.006	1	U3
230311_s_at	PRDM6	PR domain containing 6	1.22	0.006	1	U4
1554919_s_at	FLJ21062	hypothetical protein FLJ21062	1.36	0.006	1	U3
231043_at	MGC33657	similar to hypothetical protein	1.42	0.006	1	U3
203912_s_at	DNASE1L1	deoxyribonuclease I-like 1	1.24	0.006	1	U1
1555787_at	C11orf63	chromosome 11 open reading frame 63	1.22	0.006	1	U3

1557417_s_at	RSPH10B	radial spoke head 10 homolog B (Chlamydomonas)	1.29	0.006	1	U3
219758_at	TTC26	tetratricopeptide repeat domain 26	1.34	0.006	1	U3
219455_at	FLJ21062	hypothetical protein FLJ21062	1.33	0.006	1	U3
223794_at	ARMC4	armadillo repeat containing 4	1.24	0.006	1	U3
239552_at	FLJ14712	hypothetical protein FLJ14712	1.24	0.007	1	U4
243237_at	MGC33657	similar to hypothetical protein	1.25	0.007	1	U3
209604_s_at	GATA3	GATA binding protein 3	1.50	0.007	1	U3
203184_at	FBN2	fibrillin 2 (congenital contractural arachnodactyly)	1.95	0.007	1	U4
232984_at	HYDIN	hydrocephalus inducing homolog (mouse)	1.56	0.007	1	U3
241470_x_at			1.43	0.007	1	U3
244571_s_at	TTC12	tetratricopeptide repeat domain 12	1.31	0.007	1	U3
231292_at	EID3	EP300 interacting inhibitor of differentiation 3	1.32	0.007	1	U3
221256_s_at	HDHD3	haloacid dehalogenase-like hydrolase domain containing 3	1.26	0.007	1	U3
238843_at	NPHP1	nephronophthisis 1 (juvenile)	1.22	0.008	1	U3
236085_at	CAPSL	calcyphosine-like	1.37	0.008	1	U3
1554988_at	SLC9A11	solute carrier family 9, member 11	1.17	0.008	1	U3
204346_s_at	RASSF1	Ras association (RalGDS/AF-6) domain family 1	1.34	0.008	1	U1
227716_at	UBXD5	UBX domain containing 5	1.24	0.008	1	U3
234893_s_at	LOC200383	similar to Dynein heavy chain at 16F	1.27	0.008	1	U3
201920_at	SLC20A1	solute carrier family 20 (phosphate transporter), member 1	1.18	0.008	1	U4
235800_at	HSPA12A	heat shock 70kDa protein 12A	1.22	0.008	1	U3
236222_at	C3orf15	chromosome 3 open reading frame 15	1.37	0.009	1	U3
1554147_s_at	C3orf15	chromosome 3 open reading frame 15	1.44	0.009	1	U3
217561_at	CALCA	calcitonin/calcitonin-related polypeptide, alpha	1.13	0.009	1	U4
224463_s_at	C11orf70	chromosome 11 open reading frame 70	1.67	0.009	1	U3
210162_s_at	NFATC1	nuclear factor of activated T-cells, cytoplasmic, calcineurin-dependent 1	1.17	0.009	1	U3
205905_s_at	MICA	MHC class I polypeptide-related	1.30	0.009	1	U1

		sequence A				
1561430_s_at	C3orf15	chromosome 3 open reading frame 15	1.37	0.009	1	U3
220658_s_at	ARNTL2	aryl hydrocarbon receptor nuclear translocator-like 2	1.37	0.009	1	U3
205979_at	SCGB2A1	secretoglobin, family 2A, member 1	1.12	0.010	1	U3
210279_at	GPR18	G protein-coupled receptor 18	1.17	0.010	1	U4
1562226_at	FLJ14712	hypothetical protein FLJ14712	1.32	0.010	1	U4
233516_s_at	SPAG17	sperm associated antigen 17	1.35	0.010	1	U3
1557636_a_at	LOC136288	hypothetical protein LOC136288	1.55	0.010	1	U3
239722_at	LOC134121	hypothetical protein LOC134121	1.29	0.010	1	U3
222240_s_at	ISYNA1	myo-inositol 1-phosphate synthase A1	1.37	0.01	1	U1
217529_at	POLR2J2	DNA directed RNA polymerase II polypeptide J-related	1.15	0.01	1	U3
200660_at	S100A11	S100 calcium binding protein A11	1.36	0.01	1	U1
231084_at	C10orf79	chromosome 10 open reading frame 79	1.42	0.01	1	U3
209278_s_at	TFPI2	tissue factor pathway inhibitor 2	1.54	0.01	1	U1
1557242_at	MICA	MHC class I polypeptide-related sequence A	1.30	0.01	1	U3
223305_at	MGC13379	HSPC244	1.26	0.01	1	U3
232998_at	TIGD4	tigger transposable element derived 4	1.17	0.01	1	U3
228749_at	ZDBF2	zinc finger, DBF-type containing 2	1.30	0.01	1	U3
52651_at	COL8A2	collagen, type VIII, alpha 2	1.42	0.01	1	U1

List of 86 genes significantly down-regulated in tumors of group B patients (short-term survivors) versus tumors of group A patients (long-term survivors):

Affymetrix Probeset ID	Gene symbol	Gene description	Expression fold change	p-value	Local FDR	Spot membership
209511_at	POLR2F	polymerase (RNA) II (DNA directed) polypeptide F	0.78	0.0002	1	d1
215342_s_at	RABGAP1L	RAB GTPase activating protein 1-like	0.77	0.0003	1	d1
1568870_at			0.56	0.0008	1	d1
229205_at	RHBDF1	rhomboid 5 homolog 1 (Drosophila)	0.79	0.0009	1	d3

213508_at	C14orf147	chromosome 14 open reading frame 147	0.89	0.002	1	d1
210414_at	FLRT1	fibronectin leucine rich transmembrane protein 1	0.63	0.002	1	d1
236824_at	TMEM132B	transmembrane protein 132B	0.61	0.002	1	d1
229875_at	ZDHHC22	zinc finger, DHHC-type containing 22	0.54	0.003	1	d1
1552439_s_at	MEGF11	multiple EGF-like-domains 11	0.61	0.003	1	d1
219819_s_at	MRPS28	mitochondrial ribosomal protein S28	0.86	0.003	1	d1
239450_at	NDUFV2	NADH dehydrogenase (ubiquinone) flavoprotein 2, 24kDa	0.86	0.003	1	d1
208195_at	TTN	titin	0.84	0.003	1	d1
226735_at	TAPT1	transmembrane anterior posterior transformation 1	0.79	0.004	1	d2
230581_at			0.79	0.004	1	d1
228764_s_at	MDP-1	magnesium-dependent phosphatase 1	0.84	0.004	1	d1
201886_at	WDR23	WD repeat domain 23	0.82	0.004	1	d1
219645_at	CASQ1	calsequestrin 1 (fast-twitch, skeletal muscle)	0.68	0.004	1	d1
220867_s_at	SLC24A2	solute carrier family 24 (sodium/potassium/calcium exchanger), member 2	0.82	0.004	1	d1
237973_at			0.76	0.004	1	d1
1559992_a_at	LOC728755	hypothetical protein LOC728755	0.60	0.004	1	d1
235072_s_at			0.88	0.004	1	d1
230994_at	MGC33846	hypothetical protein MGC33846	0.88	0.004	1	d1
1556971_a_at	SLC25A28	solute carrier family 25, member 28	0.87	0.004	1	d1
236468_at			0.64	0.004	1	d1
227933_at	LINGO1	leucine rich repeat and Ig domain containing 1	0.81	0.004	1	d3
219547_at	COX15	COX15 homolog, cytochrome c oxidase assembly protein (yeast)	0.87	0.004	1	d1
226232_at			0.85	0.005	1	d3
203260_at	HDDC2	HD domain containing 2	0.80	0.005	1	d1
205643_s_at	PPP2R2B	protein phosphatase 2 (formerly 2A), regulatory subunit B, beta isoform	0.84	0.005	1	d1
230244_at	UNQ830	ASCL830	0.60	0.005	1	d1

236688_at	FRMPD3	FERM and PDZ domain containing 3	0.69	0.006	1	d3
217337_at	LOC646677	similar to aconitase 2, mitochondrial	0.78	0.006	1	d1
206192_at	CDSN	corneodesmosin	0.87	0.006	1	d1
212970_at			0.86	0.006	1	d3
232069_at	KIF26A	kinesin family member 26A	0.72	0.006	1	d1
223605_at	SLC25A18	solute carrier family 25 (mitochondrial carrier), member 18	0.74	0.006	1	d1
214460_at	LSAMP	limbic system-associated membrane protein	0.79	0.007	1	d3
233496_s_at	CFL2	cofilin 2 (muscle)	0.86	0.007	1	d2
222780_s_at	BAALC	brain and acute leukemia, cytoplasmic	0.82	0.007	1	d1
58308_at	TRIM62	tripartite motif-containing 62	0.85	0.007	1	d3
243969_at	SLC24A4	solute carrier family 24 (sodium/potassium/calcium exchanger), member 4	0.64	0.007	1	d1
231372_at	LOC153328	similar to CG4995 gene product	0.64	0.007	1	d1
238389_s_at			0.85	0.007	1	d1
1552694_at	SLC2A13	solute carrier family 2 (facilitated glucose transporter), member 13	0.74	0.007	1	d1
57588_at	SLC24A3	solute carrier family 24 (sodium/potassium/calcium exchanger), member 3	0.77	0.007	1	d1
238442_at	HEXIM1	hexamethylene bis-acetamide inducible 1	0.84	0.007	1	d1
238650_x_at	WDR89	WD repeat domain 89	0.89	0.007	1	d1
244780_at	SGPP2	sphingosine-1-phosphate phosphotase 2	0.75	0.008	1	d1
231508_s_at			0.86	0.008	1	d1
215358_x_at	ZNF37B	zinc finger protein 37B	0.82	0.008	1	d1
234988_at	VCPIP1	valosin containing protein (p97)/p47 complex interacting protein 1	0.86	0.008	1	d1
213419_at	APBB2	amyloid beta (A4) precursor protein-binding, family B, member 2 (Fe65-like)	0.82	0.009	1	d1
206615_s_at	ADAM22	ADAM metallopeptidase domain 22	0.73	0.009	1	d2
209135_at	ASPH	aspartate beta-hydroxylase	0.90	0.009	1	d3
219300_s_at	CNTNAP2	contactin associated protein-like 2	0.71	0.009	1	d1

1552695_a_at	SLC2A13	solute carrier family 2 (facilitated glucose transporter), member 13	0.72	0.009	1	d1
224663_s_at	CFL2	cofilin 2 (muscle)	0.92	0.009	1	d1
218899_s_at	BAALC	brain and acute leukemia, cytoplasmic	0.85	0.009	1	d1
231302_at			0.80	0.009	1	d1
217092_x_at	LOC646912	similar to 60S ribosomal protein L7	0.87	0.009	1	d1
221378_at	CER1	cerberus 1, cysteine knot superfamily, homolog (Xenopus laevis)	0.87	0.009	1	d1
225913_at	SGK269	NKF3 kinase family member	0.91	0.009	1	d3
1557232_at			0.86	0.010	1	d3
1553268_at	RHBDL3	rhomboid, veinlet-like 3 (Drosophila)	0.66	0.010	1	d1
240332_at			0.84	0.010	1	d1
231512_at			0.80	0.010	1	d1
204521_at	C12orf24	chromosome 12 open reading frame 24	0.89	0.010	1	d1
222957_at	NEU4	sialidase 4	0.70	0.010	1	d1
213369_at	PCDH21	protocadherin 21	0.64	0.01	1	d1
240471_at	SENP1	SUMO1/sentrin specific peptidase 1	0.90	0.01	1	d1
1558790_s_at	C8orf77	chromosome 8 open reading frame 77	0.91	0.01	1	d1
206453_s_at	NDRG2	NDRG family member 2	0.77	0.01	1	d1
217244_at			0.90	0.01	1	d1
213265_at	PGA3	pepsinogen 3, group I (pepsinogen A)	0.80	0.01	1	d1
202964_s_at	RFX5	regulatory factor X, 5 (influences HLA class II expression)	0.88	0.01	1	d1
222171_s_at	PKNOX2	PBX/knotted 1 homeobox 2	0.76	0.01	1	d3
228942_s_at	DAB2IP	DAB2 interacting protein	0.86	0.01	1	d3
206993_at	ATP5S	ATP synthase, H+ transporting, mitochondrial F0 complex, subunit s (factor B)	0.80	0.01	1	d1
219090_at	SLC24A3	solute carrier family 24 (sodium/potassium/calcium exchanger), member 3	0.75	0.01	1	d1
235025_at	WDR89	WD repeat domain 89	0.87	0.01	1	d2
219060_at	C8orf32	chromosome 8 open reading frame 32	0.91	0.01	1	d1

1558733_at	ZBTB38	zinc finger and BTB domain containing 38	0.85	0.01	1	d2
243984_at			0.72	0.01	1	d1
242342_at			0.74	0.01	1	d1
219701_at	TMOD2	tropomodulin 2 (neuronal)	0.78	0.01	1	d1
223754_at	MGC13057	hypothetical protein MGC13057	0.79	0.01	1	d1

Supplementary Table 4. List of genes showing differential expression between *IDH1/2*-wildtype and *IDH1/2*-mutant glioblastomas of our series. Genes were selected using the same criteria as described in the legend to Supplementary Table 3.

List of 138 genes up-regulated in *IDH1/2*^{wt} relative to *IDH1/2*^{mut} glioblastomas:

Affymetrix Probeset ID	Gene symbol	Gene description	Expression fold change	p-value	Local FDR	Spot membership
221898_at	PDPN	podoplanin	3.18	10^{-09}	0.0002	U1
213340_s_at	KIAA0495	KIAA0495	2.02	10^{-08}	0.0004	U1
209395_at	CHI3L1	chitinase 3-like 1 (cartilage glycoprotein-39)	3.49	10^{-08}	0.0005	U1
213113_s_at	SLC43A3	solute carrier family 43, member 3	1.87	10^{-08}	0.0008	U1
226658_at	PDPN	podoplanin	3.38	10^{-08}	0.0009	U1
209396_s_at	CHI3L1	chitinase 3-like 1 (cartilage glycoprotein-39)	4.30	10^{-08}	0.001	U1
200600_at	MSN	moesin	1.54	10^{-07}	0.002	U1
225286_at	ARSD	arylsulfatase D	2.12	10^{-07}	0.002	U1
204879_at	PDPN	podoplanin	3.48	10^{-07}	0.003	U1
209356_x_at	EFEMP2	EGF-containing fibulin-like extracellular matrix protein 2	2.27	10^{-06}	0.005	U1
223696_at	ARSD	arylsulfatase D	1.92	10^{-06}	0.005	U1
222640_at	DNMT3A	DNA (cytosine-5-)-methyltransferase 3 alpha	1.56	10^{-06}	0.005	U2
206025_s_at	TNFAIP6	tumor necrosis factor, alpha-induced protein 6	3.16	10^{-06}	0.005	U1
220233_at	FBXO17	F-box protein 17	2.25	10^{-06}	0.005	U1
201666_at	TIMP1	TIMP metallopeptidase inhibitor 1	2.23	10^{-06}	0.007	U1
208659_at	CLIC1	chloride intracellular channel 1	1.78	10^{-06}	0.007	U1
1557051_s_at	HOXA2	homeobox A2	2.78	10^{-06}	0.008	U1
224874_at	POLR1D	polymerase (RNA) I polypeptide D, 16kDa	1.41	10^{-06}	0.008	U1
200916_at	TAGLN2	transgelin 2	1.83	10^{-06}	0.009	U1
235940_at	C9orf64	chromosome 9 open reading frame 64	1.70	10^{-06}	0.01	U1
212169_at	FKBP9	FK506 binding protein 9, 63 kDa	1.47	10^{-06}	0.01	U1
243931_at	CD58	CD58 molecule	2.10	10^{-06}	0.01	U1
203729_at	EMP3	epithelial membrane protein 3	1.89	10^{-06}	0.01	U1
225434_at	DEDD2	death effector domain containing 2	1.47	10^{-06}	0.01	U1
218802_at	CCDC109B	coiled-coil domain containing 109B	1.85	10^{-06}	0.01	U1
228642_at	HOXA2	homeobox A2	3.71	10^{-06}	0.02	U1
201792_at	AEBP1	AE binding protein 1	2.21	10^{-06}	0.02	U1
222757_s_at	ZAK	sterile alpha motif and leucine zipper containing kinase AZK	1.77	10^{-05}	0.02	U1
222150_s_at	tcag7.1314	hypothetical protein LOC54103	1.66	10^{-05}	0.02	U1
212356_at	KIAA0323	KIAA0323	1.71	10^{-05}	0.02	U1

1569898_a_at			2.07	10^{-05}	0.02	U1
201136_at	PLP2	proteolipid protein 2 (colonic epithelium-enriched)	1.77	10^{-05}	0.02	U1
225128_at	KDELC2	KDEL (Lys-Asp-Glu-Leu) containing 2	1.57	10^{-05}	0.02	U1
213142_x_at	tcag7.1314	hypothetical protein LOC54103	1.59	10^{-05}	0.02	U1
202718_at	IGFBP2	insulin-like growth factor binding protein 2, 36kDa	2.51	10^{-05}	0.02	U1
208782_at	FSTL1	follistatin-like 1	1.52	10^{-05}	0.02	U1
244533_at			1.72	10^{-05}	0.03	U1
213556_at	LOC390940	similar to R28379_1	1.94	10^{-05}	0.03	U1
224710_at	RAB34	RAB34, member RAS oncogene family	2.44	10^{-05}	0.03	U1
1555630_a_at	RAB34	RAB34, member RAS oncogene family	2.31	10^{-05}	0.03	U1
221024_s_at	SLC2A10	solute carrier family 2 (facilitated glucose transporter), member 10	1.91	10^{-05}	0.03	U1
218950_at	CENTD3	centaurin, delta 3	1.68	10^{-05}	0.03	U1
225612_s_at	B3GNT5	UDP-GlcNAc:betaGal beta-1,3-N-acetylglucosaminyltransferase 5	1.74	10^{-05}	0.03	U1
210978_s_at	TAGLN2	transgelin 2	1.82	10^{-05}	0.03	U1
204348_s_at	AK3L1	adenylate kinase 3-like 1	1.76	10^{-05}	0.04	U1
206580_s_at	EFEMP2	EGF-containing fibulin-like extracellular matrix protein 2	1.56	10^{-05}	0.04	U1
222217_s_at	SLC27A3	solute carrier family 27 (fatty acid transporter), member 3	1.76	10^{-05}	0.04	U1
221664_s_at	F11R	F11 receptor	1.66	10^{-05}	0.04	U1
223380_s_at	LATS2	LATS, large tumor suppressor, homolog 2 (Drosophila)	1.50	10^{-05}	0.05	U1
226670_s_at	C20orf119	chromosome 20 open reading frame 119	1.80	10^{-05}	0.05	U1
226777_at			2.37	10^{-05}	0.05	U1
230630_at			1.93	10^{-05}	0.05	U1
223120_at	FUCA2	fucosidase, alpha-L- 2, plasma	1.74	10^{-05}	0.05	U1
204363_at	F3	coagulation factor III (thromboplastin, tissue factor)	1.48	10^{-05}	0.05	U1
205173_x_at	CD58	CD58 molecule	1.73	10^{-05}	0.05	U1
1558527_at			1.99	10^{-05}	0.05	U1
208816_x_at	ANXA2P2	annexin A2 pseudogene 2	1.82	10^{-05}	0.05	U1
204741_at	BICD1	bicaudal D homolog 1 (Drosophila)	1.34	10^{-05}	0.05	U1
212355_at	KIAA0323	KIAA0323	2.07	10^{-05}	0.05	U1
203819_s_at	C7orf30	chromosome 7 open reading frame 30	2.83	10^{-05}	0.06	U1
219890_at	CLEC5A	C-type lectin domain family 5, member A	3.36	10^{-05}	0.06	U1
224950_at	PTGFRN	prostaglandin F2 receptor negative regulator	1.73	10^{-05}	0.06	U1
217966_s_at	FAM129A	family with sequence similarity 129, member A	1.99	10^{-05}	0.06	U1

208790_s_at	PTRF	polymerase I and transcript release factor	2.29	10^{-05}	0.06	U1
209164_s_at	CYB561	cytochrome b-561	1.65	10^{-05}	0.06	U1
202208_s_at	ARL4C	ADP-ribosylation factor-like 4C	1.61	10^{-05}	0.06	U1
203409_at	DDB2	damage-specific DNA binding protein 2, 48kDa	2.41	10^{-05}	0.06	U1
37408_at	MRC2	mannose receptor, C type 2	1.62	0.0001	0.07	U1
208789_at	PTRF	polymerase I and transcript release factor	1.47	0.0001	0.07	U1
200771_at	LAMC1	laminin, gamma 1 (formerly LAMB2)	1.40	0.0001	0.07	U1
213644_at	CCDC46	coiled-coil domain containing 46	1.58	0.0001	0.07	U1
202990_at	PYGL	phosphorylase, glycogen; liver (Hers disease, glycogen storage disease type VI)	1.56	0.0001	0.07	U1
218618_s_at	FNDC3B	fibronectin type III domain containing 3B	1.41	0.0001	0.07	U1
201012_at	ANXA1	annexin A1	1.70	0.0001	0.07	U1
213524_s_at	G0S2	G0/G1switch 2	2.05	0.0001	0.07	U1
210692_s_at	SLC43A3	solute carrier family 43, member 3	1.73	0.0001	0.07	U2
215870_s_at	PLA2G5	phospholipase A2, group V	3.16	0.0001	0.07	U1
236429_at	ZNF83	zinc finger protein 83	1.79	0.0001	0.07	U1
217730_at	TMBIM1	transmembrane BAX inhibitor motif containing 1	1.38	0.0001	0.08	U1
224937_at	PTGFRN	prostaglandin F2 receptor negative regulator	1.48	0.0001	0.08	U1
1556051_a_at	BICD1	bicaudal D homolog 1 (Drosophila)	1.32	0.0001	0.08	U1
201170_s_at	BHLHB2	basic helix-loop-helix domain containing, class B, 2	1.50	0.0001	0.08	U1
225314_at	OCIAD2	OCIA domain containing 2	2.63	0.0002	0.08	U1
217733_s_at	TMSB10	thymosin, beta 10	1.39	0.0002	0.08	U1
202465_at	PCOLCE	procollagen C-endopeptidase enhancer	2.09	0.0002	0.08	U1
227013_at	LATS2	LATS, large tumor suppressor, homolog 2 (Drosophila)	1.49	0.0002	0.09	U1
204485_s_at	TOM1L1	target of myb1 (chicken)-like 1	1.94	0.0002	0.09	U1
218983_at	C1RL	complement component 1, r subcomponent-like	1.72	0.0002	0.09	U1
200770_s_at	LAMC1	laminin, gamma 1 (formerly LAMB2)	1.56	0.0002	0.09	U1
230733_at	MRCL3	myosin regulatory light chain MRCL3	1.66	0.0002	0.09	U1
225799_at	LOC541471	hypothetical LOC541471	1.84	0.0002	0.09	U1
228243_at	PAXIP1	PAX interacting (with transcription-activation domain) protein 1	1.76	0.0002	0.09	U1
205918_at	SLC4A3	solute carrier family 4, anion exchanger, member 3	1.77	0.0002	0.09	U1
208637_x_at	ACTN1	actinin, alpha 1	1.62	0.0002	0.09	U1

200791_s_at	IQGAP1	IQ motif containing GTPase activating protein 1	1.39	0.0002	0.10	U1
214733_s_at	YIPF1	Yip1 domain family, member 1	1.31	0.0002	0.10	U2
225867_at	VASN	vasorin	1.80	0.0002	0.10	U1
209306_s_at	SWAP70	SWAP-70 protein	1.37	0.0002	0.10	U1
213455_at	FAM114A1	family with sequence similarity 114, member A1	1.46	0.0002	0.10	U1
213503_x_at	ANXA2	annexin A2	1.71	0.0002	0.10	U1
202856_s_at	SLC16A3	solute carrier family 16, member 3 (monocarboxylic acid transporter 4)	2.49	0.0002	0.10	U1
213790_at	ADAM12	ADAM metallopeptidase domain 12 (meltrin alpha)	2.72	0.0003	0.11	U1
200660_at	S100A11	S100 calcium binding protein A11	1.70	0.0003	0.11	U1
209909_s_at	TGFB2	transforming growth factor, beta 2	2.13	0.0003	0.11	U1
217200_x_at	CYB561	cytochrome b-561	1.46	0.0003	0.11	U1
210427_x_at	ANXA2	annexin A2	1.70	0.0003	0.11	U1
219332_at	MICALL2	MICAL-like 2	1.76	0.0003	0.11	U1
224857_s_at	POLR1D	polymerase (RNA) I polypeptide D, 16kDa	1.29	0.0003	0.11	U2
228057_at	DDIT4L	DNA-damage-inducible transcript 4-like	2.36	0.0003	0.11	U1
218424_s_at	STEAP3	STEAP family member 3	1.85	0.0003	0.11	U1
201590_x_at	ANXA2	annexin A2	1.68	0.0003	0.11	U1
210135_s_at	SHOX2	short stature homeobox 2	3.23	0.0003	0.12	U1
200650_s_at	LDHA	lactate dehydrogenase A	1.52	0.0003	0.12	U1
202669_s_at	EFNB2	ephrin-B2	1.70	0.0003	0.12	U1
202709_at	FMOD	fibromodulin	2.70	0.0003	0.12	U1
201105_at	LGALS1	lectin, galactoside-binding, soluble, 1 (galectin 1)	1.54	0.0003	0.12	U1
217967_s_at	FAM129A	family with sequence similarity 129, member A	1.66	0.0003	0.12	U1
1557938_s_at	PTRF	polymerase I and transcript release factor	1.62	0.0004	0.12	U1
232423_at	ARSD	arylsulfatase D	1.84	0.0004	0.13	U1
228141_at	LOC493869	similar to RIKEN cDNA 2310016C16	2.20	0.0004	0.13	U1
203234_at	UPP1	uridine phosphorylase 1	1.86	0.0004	0.13	U1
213418_at	HSPA6	heat shock 70kDa protein 6 (HSP70B')	2.48	0.0004	0.13	U1
207667_s_at	MAP2K3	mitogen-activated protein kinase kinase 3	1.65	0.0004	0.13	U1
213812_s_at	CAMKK2	calcium/calmodulin-dependent protein kinase kinase 2, beta	1.30	0.0004	0.13	U1
200782_at	ANXA5	annexin A5	1.30	0.0004	0.13	U1
225173_at	ARHGAP18	Rho GTPase activating protein 18	1.86	0.0004	0.13	U1
210840_s_at	IQGAP1	IQ motif containing GTPase activating protein 1	1.41	0.0004	0.13	U1
226122_at	PLEKHG1	pleckstrin homology domain containing, family G (with RhoGef domain) member 1	1.49	0.0004	0.13	U1

209129_at	TRIP6	thyroid hormone receptor interactor 6	1.46	0.0004	0.13	U1
202269_x_at	GBP1	guanylate binding protein 1, interferon-inducible, 67kDa	1.66	0.0004	0.13	U1
1554600_s_at	LMNA	lamin A/C	1.41	0.0004	0.13	U1
201860_s_at	PLAT	plasminogen activator, tissue	1.70	0.0004	0.13	U1
210137_s_at	DCTD	dCMP deaminase	1.45	0.0004	0.13	U1
211160_x_at	ACTN1	actinin, alpha 1	1.77	0.0004	0.14	U1
225342_at	AK3L1	adenylate kinase 3-like 1	1.51	0.0004	0.14	U1
207714_s_at	SERPINH1	serpin peptidase inhibitor, clade H (heat shock protein 47), member 1, (collagen binding protein 1)	2.30	0.0004	0.14	U1
202952_s_at	ADAM12	ADAM metallopeptidase domain 12 (meltrin alpha)	2.17	0.0005	0.14	U1
202207_at	ARL4C	ADP-ribosylation factor-like 4C	1.43	0.0005	0.14	U2

List of 124 genes down-regulated in *IDH1/2*^{wt} relative to *IDH1/2*^{mut} glioblastomas:

Affymetrix Probeset ID	Gene symbol	Gene description	Expression fold change	p-value	Local FDR	Spot membership
1553344_at	PCDH15	protocadherin 15	0.49	10^{-07}	0.02	d1
230307_at	SLC25A21	solute carrier family 25 (mitochondrial oxodicarboxylate carrier), member 21	0.48	10^{-06}	0.02	d1
233136_at	PABPC5	poly(A) binding protein, cytoplasmic 5	0.36	10^{-06}	0.02	d1
234124_at	SH3D19	SH3 domain protein D19	0.44	10^{-06}	0.02	d1
237525_at			0.59	10^{-06}	0.03	d1
244767_at			0.64	10^{-06}	0.03	d1
232487_at	SFT2D1	SFT2 domain containing 1	0.54	10^{-06}	0.03	d1
219661_at	RANBP17	RAN binding protein 17	0.44	10^{-06}	0.03	d1
212453_at	KIAA1279	KIAA1279	0.78	10^{-05}	0.04	d1
205705_at	ANKRD26	ankyrin repeat domain 26	0.56	10^{-05}	0.05	d1
242571_at	REPS2	RALBP1 associated Eps domain containing 2	0.45	10^{-05}	0.05	d1
244198_at	RANBP17	RAN binding protein 17	0.72	10^{-05}	0.05	d1
229590_at	RPL13	ribosomal protein L13	0.55	10^{-05}	0.05	d1
218878_s_at	SIRT1	sirtuin (silent mating type information regulation 2 homolog) 1 (S. cerevisiae)	0.75	10^{-05}	0.06	d1
1556808_at	LOC121906	similar to Proteasome subunit alpha type 6 (Proteasome iota chain) (Macropain iota chain) (Multicatalytic endopeptidase complex iota chain)	0.58	10^{-05}	0.06	d1
1554281_at			0.37	10^{-05}	0.06	d1
236771_at	C6orf159	chromosome 6 open reading frame 159	0.48	10^{-05}	0.06	d1
240228_at	CSMD3	CUB and Sushi multiple domains 3	0.35	10^{-05}	0.06	d1

1554547_at	FAM13C1	family with sequence similarity 13, member C1	0.68	10^{-05}	0.06	d1
218970_s_at	CUTC	cutC copper transporter homolog (E. coli)	0.74	10^{-05}	0.06	d1
232803_at	FLJ31958	hypothetical protein FLJ31958	0.63	10^{-05}	0.06	d1
226680_at	IKZF5	IKAROS family zinc finger 5 (Pegasus)	0.72	10^{-05}	0.07	d1
205747_at	CBLN1	cerebellin 1 precursor	0.62	10^{-05}	0.07	d1
225663_at	ACBD5	acyl-Coenzyme A binding domain containing 5	0.77	10^{-05}	0.07	d1
205773_at	CPEB3	cytoplasmic polyadenylation element binding protein 3	0.63	10^{-05}	0.07	d1
225497_at	ATE1	arginyltransferase 1	0.77	10^{-05}	0.07	d1
219336_s_at	ASCC1	activating signal cointegrator 1 complex subunit 1	0.78	10^{-05}	0.07	d1
209379_s_at	KIAA1128	KIAA1128	0.79	10^{-05}	0.07	d1
1558706_a_at	ATOH8	atonal homolog 8 (Drosophila)	0.43	10^{-05}	0.07	d1
233546_at	LOC283075	hypothetical protein LOC283075	0.52	10^{-05}	0.07	d1
212905_at	CSTF2T	cleavage stimulation factor, 3' pre-RNA, subunit 2, 64kDa, tau variant	0.78	10^{-05}	0.07	d1
229234_at	ZC3H12B	zinc finger CCCH-type containing 12B	0.42	10^{-05}	0.07	d1
222390_at	WAC	WW domain containing adaptor with coiled-coil	0.83	10^{-05}	0.07	d1
235591_at	SSTR1	somatostatin receptor 1	0.46	10^{-05}	0.08	d1
213224_s_at	LOC92482	hypothetical protein LOC92482	0.75	10^{-05}	0.08	d1
1562583_s_at	LOC646405	hypothetical LOC646405	0.58	10^{-05}	0.08	d1
1553354_a_at	FLJ31958	hypothetical protein FLJ31958	0.67	10^{-05}	0.08	d1
227585_at			0.57	10^{-05}	0.08	d1
231977_at	GRID1	glutamate receptor, ionotropic, delta 1	0.56	10^{-05}	0.08	d1
225130_at	ZRANB1	zinc finger, RAN-binding domain containing 1	0.64	10^{-05}	0.08	d1
239637_at	RAB18	RAB18, member RAS oncogene family	0.64	10^{-05}	0.08	d1
218590_at	PEO1	progressive external ophthalmoplegia 1	0.62	10^{-05}	0.08	d1
1569348_at	psiTPTE22	TPTE pseudogene	0.53	10^{-05}	0.08	d1
225585_at	RAP2A	RAP2A, member of RAS oncogene family	0.71	10^{-05}	0.08	d1
239863_at			0.61	10^{-05}	0.08	d1
231053_at			0.57	10^{-05}	0.09	d1
212267_at	WAPAL	wings apart-like homolog (Drosophila)	0.86	10^{-05}	0.09	d1
234110_at	LOC283075	hypothetical protein LOC283075	0.76	0.0001	0.09	d1
239787_at	KCTD4	potassium channel tetramerisation domain containing 4	0.54	0.0001	0.09	d1
1552427_at	ZNF485	zinc finger protein 485	0.64	0.0001	0.09	d1
230575_at	MSRB2	methionine sulfoxide reductase B2	0.72	0.0001	0.09	d1

217742_s_at	WAC	WW domain containing adaptor with coiled-coil	0.83	0.0001	0.09	d1
223336_s_at	RAB18	RAB18, member RAS oncogene family	0.76	0.0001	0.09	d1
202136_at	ZMYND11	zinc finger, MYND domain containing 11	0.81	0.0001	0.09	d1
231805_at	PRLHR	prolactin releasing hormone receptor	0.49	0.0001	0.09	d1
202641_at	ARL3	ADP-ribosylation factor-like 3	0.78	0.0001	0.09	d1
224763_at	RPL37	ribosomal protein L37	0.73	0.0001	0.09	d1
1565644_at	LOC143286	hypothetical protein LOC143286	0.59	0.0001	0.10	d1
243804_at	MTMR7	myotubularin related protein 7	0.54	0.0001	0.10	d1
224755_at			0.77	0.0001	0.10	d1
222794_x_at	PAPD1	PAP associated domain containing 1	0.83	0.0001	0.10	d1
1570120_at			0.40	0.0001	0.10	d1
1554592_a_at	SLC1A6	solute carrier family 1 (high affinity aspartate/glutamate transporter), member 6	0.45	0.0001	0.10	d1
244246_at	MIPOL1	mirror-image polydactyly 1	0.50	0.0001	0.10	d1
218297_at	C10orf97	chromosome 10 open reading frame 97	0.76	0.0002	0.10	d1
213896_x_at	KIAA0974	KIAA0974	0.72	0.0002	0.10	d1
209028_s_at	ABI1	abl-interactor 1	0.79	0.0002	0.10	d1
1555958_at	CRTAC1	cartilage acidic protein 1	0.36	0.0002	0.10	d1
214914_at	FAM13C1	family with sequence similarity 13, member C1	0.69	0.0002	0.10	d1
215112_x_at	MCF2L2	MCF.2 cell line derived transforming sequence-like 2	0.72	0.0002	0.11	d1
212462_at	MYST4	MYST histone acetyltransferase (monocytic leukemia) 4	0.80	0.0002	0.11	d1
231131_at	FAM133A	family with sequence similarity 133, member A	0.41	0.0002	0.11	d1
1554702_at	NALCN	sodium leak channel, non-selective	0.60	0.0002	0.11	d1
1554593_s_at	SLC1A6	solute carrier family 1 (high affinity aspartate/glutamate transporter), member 6	0.40	0.0002	0.11	d1
1552573_s_at	MIPOL1	mirror-image polydactyly 1	0.60	0.0002	0.11	d1
216903_s_at	CBARA1	calcium binding atopy-related autoantigen 1	0.77	0.0002	0.11	d1
213549_at			0.79	0.0002	0.11	d1
227781_x_at	FAM57B	family with sequence similarity 57, member B	0.60	0.0002	0.11	d1
212989_at	SGMS1	sphingomyelin synthase 1	0.65	0.0002	0.11	d1
230350_at			0.80	0.0002	0.11	d3
206355_at	GNAL	guanine nucleotide binding protein (G protein), alpha activating activity polypeptide, olfactory type	0.46	0.0002	0.11	d1
236887_at	KIN	KIN, antigenic determinant of recA protein homolog (mouse)	0.62	0.0002	0.12	d1
221763_at	JMJD1C	jumonji domain containing 1C	0.79	0.0002	0.12	d1

206356_s_at	GNAL	guanine nucleotide binding protein (G protein), alpha activating activity polypeptide, olfactory type	0.54	0.0002	0.12	d1
228509_at	SKIP	SPHK1 (sphingosine kinase type 1) interacting protein	0.35	0.0003	0.12	d1
1562389_at			0.58	0.0003	0.12	d1
235164_at	ZNF25	zinc finger protein 25	0.73	0.0003	0.12	d1
242418_at	LOC730719	similar to Protein neurobeachin (Lysosomal trafficking regulator 2) (Protein BCL8B)	0.57	0.0003	0.12	d1
1556078_at	LOC143286	hypothetical protein LOC143286	0.77	0.0003	0.12	d1
230979_at			0.65	0.0003	0.12	d1
225950_at	SAMD8	sterile alpha motif domain containing 8	0.78	0.0003	0.12	d1
236197_at	NCBP1	nuclear cap binding protein subunit 1, 80kDa	0.71	0.0003	0.12	d1
202364_at	MXI1	MAX interactor 1	0.76	0.0003	0.13	d1
1558705_at	ATOH8	atonal homolog 8 (Drosophila)	0.68	0.0003	0.13	d1
213463_s_at	KIAA0974	KIAA0974	0.79	0.0003	0.13	d1
215473_at	LOC645256	similar to Glyceraldehyde-3-phosphate dehydrogenase (GAPDH)	0.50	0.0003	0.13	d1
240512_x_at	KCTD4	potassium channel tetramerisation domain containing 4	0.63	0.0003	0.13	d1
238739_at			0.74	0.0003	0.13	d1
235747_at	SLC25A16	solute carrier family 25 (mitochondrial carrier; Graves disease autoantigen), member 16	0.69	0.0003	0.13	d1
1561479_at			0.60	0.0003	0.13	d1
212503_s_at	DIP2C	DIP2 disco-interacting protein 2 homolog C (Drosophila)	0.75	0.0004	0.13	d1
1557775_a_at	RANBP17	RAN binding protein 17	0.80	0.0004	0.13	d1
226634_at	LOC399818	similar to CG9643-PA	0.66	0.0004	0.13	d1
1556062_at	RPP30	ribonuclease P/MRP 30kDa subunit	0.63	0.0004	0.13	d1
205645_at	REPS2	RALBP1 associated Eps domain containing 2	0.57	0.0004	0.13	d1
204615_x_at	IDI1	isopentenyl-diphosphate delta isomerase 1	0.76	0.0004	0.13	d1
218264_at	BCCIP	BRCA2 and CDKN1A interacting protein	0.76	0.0004	0.13	d1
236576_at			0.46	0.0004	0.13	d1
224780_at	RBM17	RNA binding motif protein 17	0.79	0.0004	0.13	d1
239738_at	DACH2	dachshund homolog 2 (Drosophila)	0.45	0.0004	0.14	d1
226623_at	PHYHIPL	phytanoyl-CoA 2-hydroxylase interacting protein-like	0.64	0.0004	0.14	d1
1558046_x_at	LOC441528	hypothetical protein LOC441528	0.64	0.0004	0.14	d1
243952_at	psiTPTE22	TPTE pseudogene	0.47	0.0004	0.14	d1

203620_s_at	FCHSD2	FCH and double SH3 domains 2	0.79	0.0004	0.14	d1
205359_at	AKAP6	A kinase (PRKA) anchor protein 6	0.53	0.0004	0.14	d1
212500_at	C10orf22	chromosome 10 open reading frame 22	0.80	0.0004	0.14	d1
1558045_a_at	LOC441528	hypothetical protein LOC441528	0.48	0.0004	0.14	d1
233469_at	psiTPTE22	TPTE pseudogene	0.65	0.0004	0.14	d1
1554143_a_at	SUGT1L1	SGT1, suppressor of G2 allele of SKP1 like 1 (S. cerevisiae)	0.68	0.0004	0.14	d1
221476_s_at	RPL15	ribosomal protein L15	0.85	0.0005	0.14	d1
236734_at	SLITRK1	SLIT and NTRK-like family, member 1	0.36	0.0005	0.15	d1
211951_at	NOLC1	nucleolar and coiled-body phosphoprotein 1	0.87	0.0005	0.15	d1
220815_at	CTNNA3	catenin (cadherin-associated protein), alpha 3	0.56	0.0005	0.15	d1
213369_at	PCDH21	protocadherin 21	0.46	0.0005	0.15	d1

Supplementary Table 5. List of genes differentially expressed between *IDH1/2*^{wt} glioblastomas from short-term survivors (group B^{wt}) and long-term survivors (group A^{wt}). Genes were selected using the same criteria as described in the legend to Supplementary Table 3.

List of 54 genes up-regulated in tumors of group **B^{wt} versus tumors of group A^{wt} patients:**

Affymetrix Probeset ID	Gene symbol	Gene description	Expression fold change	p-value	Local FDR	Spot membership
231472_at	FBXO15	F-box protein 15	1.50	10^{-05}	0.32	U3
240261_at	TOM1L1	target of myb1 (chicken)-like 1	1.41	10^{-05}	0.33	U3
229146_at	C7orf31	chromosome 7 open reading frame 31	1.38	10^{-05}	0.34	U3
203184_at	FBN2	fibrillin 2 (congenital contractural arachnodactyly)	2.47	10^{-05}	0.37	U4
231018_at	LOC342979	hypothetical LOC342979	1.38	0.0001	0.41	U3
236255_at	KIAA1909	KIAA1909 protein	1.48	0.0001	0.42	U3
223817_at	LRRIQ1	leucine-rich repeats and IQ motif containing 1	1.35	0.0002	0.44	U3
243957_at	LOC400464	similar to FLJ43276 protein	1.38	0.0002	0.48	U3
229782_at	RMST	rhabdomyosarcoma 2 associated transcript (non-coding RNA)	1.86	0.0002	0.48	U3
238116_at	DYNLRB2	dynein, light chain, roadblock-type 2	1.75	0.0003	0.49	U3
224463_s_at	C11orf70	chromosome 11 open reading frame 70	1.95	0.0004	0.52	U3
243237_at	MGC33657	similar to hypothetical protein	1.31	0.0004	0.52	U3
223624_at	ANUBL1	AN1, ubiquitin-like, homolog (Xenopus laevis)	1.25	0.0004	0.54	U3
220144_s_at	ANKRD5	ankyrin repeat domain 5	1.38	0.0005	0.55	U3
1563638_at	FAM18A	family with sequence similarity 18, member A	1.54	0.0005	0.56	U3
241198_s_at	C11orf70	chromosome 11 open reading frame 70	1.49	0.0006	0.56	U3
222325_at	RMST	rhabdomyosarcoma 2 associated transcript (non-coding RNA)	1.73	0.0007	0.58	U3
222068_s_at	LRRC50	leucine rich repeat containing 50	1.33	0.0007	0.58	U3
1559086_at	LOC344595	hypothetical LOC344595	1.12	0.0008	0.59	U3
222773_s_at	GALNT12	UDP-N-acetyl-alpha-D-galactosamine:polypeptide N-acetylgalactosaminyltransferase 12 (GalNAc-T12)	1.25	0.001	0.62	U4
231043_at	MGC33657	similar to hypothetical protein	1.49	0.001	0.63	U3
233907_s_at			1.23	0.001	0.63	U4
236085_at	CAPSL	calcyphosine-like	1.46	0.001	0.63	U3
210731_s_at			1.14	0.001	0.64	U4

229912_at	SDK1	sidekick homolog 1, cell adhesion molecule (chicken)	1.43	0.001	0.65	U3
228660_x_at	SEMA4F	sema domain, immunoglobulin domain (Ig), transmembrane domain (TM) and short cytoplasmic domain, (semaphorin) 4F	1.32	0.001	0.65	U4
220520_s_at	NUP62CL	nucleoporin 62kDa C-terminal like	1.29	0.001	0.65	U3
223794_at	ARMC4	armadillo repeat containing 4	1.28	0.002	0.66	U3
225701_at	AKNA	AT-hook transcription factor	1.32	0.002	0.66	U3
234893_s_at	LOC200383	similar to Dynein heavy chain at 16F	1.32	0.002	0.67	U3
231909_x_at	ODF2L	outer dense fiber of sperm tails 2-like	1.24	0.002	0.67	U3
1562301_at	C8orf34	chromosome 8 open reading frame 34	1.33	0.002	0.68	U3
230976_at	C9orf98	chromosome 9 open reading frame 98	1.31	0.002	0.69	U3
232998_at	TIGD4	tigger transposable element derived 4	1.20	0.002	0.70	U3
1554919_s_at	FLJ21062	hypothetical protein FLJ21062	1.39	0.002	0.70	U3
209656_s_at	TMEM47	transmembrane protein 47	1.22	0.002	0.70	U3
1557417_s_at	RSPH10B	radial spoke head 10 homolog B (Chlamydomonas)	1.32	0.003	0.71	U3
1553829_at	C2orf58	chromosome 2 open reading frame 58	1.12	0.003	0.71	U4
219455_at	FLJ21062	hypothetical protein FLJ21062	1.34	0.003	0.72	U3
233353_at	FER1L5	fer-1-like 5 (C. elegans)	1.13	0.003	0.72	U3
243978_at	C20orf175	chromosome 20 open reading frame 175	1.13	0.003	0.72	U4
224698_at	FAM62B	family with sequence similarity 62 (C2 domain containing) member B	1.10	0.003	0.72	U3
215598_at	TTC12	tetratricopeptide repeat domain 12	1.18	0.003	0.72	U3
231773_at	ANGPTL1	angiopoietin-like 1	1.57	0.003	0.72	U3
235559_at	FLJ22374	hypothetical protein FLJ22374	1.27	0.003	0.73	U3
229973_at	C1orf173	chromosome 1 open reading frame 173	1.58	0.003	0.73	U3
228213_at	H2AFJ	H2A histone family, member J	1.22	0.003	0.73	U3
216782_at	KCNJ15	potassium inwardly-rectifying channel, subfamily J, member 15	1.11	0.003	0.73	U4
230311_s_at	PRDM6	PR domain containing 6	1.21	0.003	0.73	U4

222089_s_at	C16orf71	chromosome 16 open reading frame 71	1.17	0.003	0.73	U3
205848_at	GAS2	growth arrest-specific 2	1.44	0.003	0.73	U4
232984_at	HYDIN	hydrocephalus inducing homolog (mouse)	1.61	0.003	0.74	U3
223305_at	MGC13379	HSPC244	1.30	0.004	0.74	U3
1555804_a_at	YSK4	yeast Sps1/Ste20-related kinase 4 (S. cerevisiae)	1.46	0.004	0.74	U3

List of 30 genes down-regulated intumors of group **B^{wt} versus tumors of group A^{wt} patients:**

Affymetrix Probeset ID	Gene symbol	Gene description	Expression fold change	p-value	Local FDR	Spot membership
235856_at	CYP21A2	cytochrome P450, family 21, subfamily A, polypeptide 2	0.64	0.0001	0.54	U2
205983_at	DPEP1	dipeptidase 1 (renal)	0.65	0.0002	0.59	U2
226028_at	ROBO4	roundabout homolog 4, magic roundabout (Drosophila)	0.81	0.0003	0.60	U2
241381_at	CXorf36	chromosome X open reading frame 36	0.74	0.0003	0.60	U2
1553768_a_at	DCBLD1	discoidin, CUB and LCCL domain containing 1	0.78	0.0003	0.61	U2
205507_at	ARHGEF15	Rho guanine nucleotide exchange factor (GEF) 15	0.80	0.0005	0.63	U2
205302_at	IGFBP1	insulin-like growth factor binding protein 1	0.66	0.0007	0.64	U2
241869_at	APOL6	apolipoprotein L, 6	0.72	0.0008	0.65	U2
236991_at			0.85	0.0009	0.66	U2
236926_at	TBX1	T-box 1	0.74	0.0010	0.66	U2
226955_at	AFAP1L1	actin filament associated protein 1-like 1	0.72	0.001	0.68	U2
230061_at	TM4SF18	transmembrane 4 L six family member 18	0.79	0.002	0.68	U2
206236_at	GPR4	G protein-coupled receptor 4	0.82	0.002	0.69	U2
226609_at	DCBLD1	discoidin, CUB and LCCL domain containing 1	0.86	0.002	0.69	U2
219656_at	PCDH12	protocadherin 12	0.75	0.002	0.69	U2
236485_at	SUZ12P	suppressor of zeste 12 homolog pseudogene	0.89	0.002	0.69	U2
202235_at	SLC16A1	solute carrier family 16, member 1 (monocarboxylic acid transporter 1)	0.87	0.002	0.70	U2
219700_at	PLXDC1	plexin domain containing 1	0.83	0.002	0.70	U2
202877_s_at	CD93	CD93 molecule	0.76	0.002	0.70	U2
1556265_at	LOC400831	hypothetical LOC400831	0.83	0.002	0.70	U2

214660_at	ITGA1	integrin, alpha 1	0.78	0.003	0.70	U2
225615_at	LOC126917	hypothetical protein LOC126917	0.82	0.003	0.71	U2
225369_at	ESAM	endothelial cell adhesion molecule	0.79	0.003	0.71	U2
235044_at	CYYR1	cysteine/tyrosine-rich 1	0.77	0.003	0.71	U2
241942_at	PXDNL	peroxidasin homolog (Drosophila)-like	0.77	0.003	0.71	U2
214428_x_at	C4A	complement component 4A (Rodgers blood group)	0.83	0.003	0.71	U2
1556314_a_at			0,75	0.003	0.71	U2
219719_at	HIGD1B	HIG1 domain family, member 1B	0.77	0.003	0.72	U2
217094_s_at	ITCH	itchy homolog E3 ubiquitin protein ligase (mouse)	0.88	0.003	0.72	U2
225973_at	TAP2	transporter 2, ATP-binding cassette, sub-family B (MDR/TAP)	0.84	0.004	0.72	U2

Supplementary Table 6. This table summarises the frequencies of gene copy number changes in different chromosomal regions of interest containing glioma-associated tumor suppressor genes or proto-oncogenes. After adjusting for multiple testing, there were not significant differences between the distinct survival groups of *IDH1/2*-wildtype glioblastoma patients (see column 'p-value *IDH1/2*^{wt}'). In contrast, significant differences were detected in the group of patients with *IDH1/2*-mutant tumors (see column 'p-value *IDH1/2*^{mut}'). The association between gene copy number in candidate genes and survival groups resp. *IDH1/2* mutation were analyzed by Fisher's exact test using IBM SPSS Statistics Version 20.

Chromosome region (hg19)	Candidate gene(s)	Group A^{wt} n=17	Group B^{wt} n=19	Group C^{wt} n=43	p-value *IDH1/2*^{wt}	Group *IDH1/2*^{mut} n=15	p-value *IDH1/2*^{mut}
Low- and high-level amplifications							
1q32.1	MDM4 (RP11-563I16), PIK3C2B (RP11-739N20)	6/15 (40%)	3/17 (18%)	16/38 (42%)	0.199	1/12 (8%)	0.092
1q44	AKT3 (RP11-269F20, RP11-370K11)	3/15 (20%)	3/16 (19%)	6/41 (15%)	0.756	1/12 (8%)	0.681
4q12	PDGFRA (RP11-231C18)	5/15 (33%)	1/16 (6%)	10/40 (25%)	0.146	2/12 (17%)	1.0
6p21.1	CCND3 (RP5-973N23, RP11-533O20)	2/15 (13%)	2/17 (12%)	2/41 (5%)	0.453	1/12 (8%)	1.0
7p22.1	PMS2 (RP11-90J23)	11/13 (85%)	13/15 (87%)	28/35 (80%)	0.906	4/11 (36%)	0.003
7p11.2	EGFR (RP5-1091E12, RP11-339F13)	14/15 (93%)	14/15 (93%)	31/33 (94%)	1.0	4/11 (36%)	<0.001
7q21.11	HGF (RP5-1098B1)	9/12 (75%)	12/13 (92%)	34/37 (92%)	0.239	5/9 (56%)	0.027
7q21.2	CDK6 (RP5-850G1)	13/14 (93%)	10/11 (91%)	34/39 (87%)	1.0	7/11 (64%)	0.050

7q31.2	MET (CTB-13N12)	11/11 (100%)	13/14 (93%)	28/35 (80%)	0.252	6/10 (60%)	0.061
13q34	SOX1 (RP11-310D8)	0/15	0/16	5/41 (12%)	0.217	3/12 (25%)	0.083
14q32.33	AKT1 (RP11-982M15)	3/12 (25%)	2/14 (14%)	11/29 (38%)	0.257	0/9	0.097
19p13.3	STK11 (RP11-50C6)	4/12 (33%)	8/15 (53%)	17/28 (61%)	0.290	4/11 (36%)	0.511
19q13.31	XRCC1 (CTB-61I7, RP11-46C6, RP11-122E7)	6/15 (40%)	5/17 (29%)	16/39 (41%)	0.758	1/12 (8%)	0.052
19q13.32	ERCC2 (RP11-43E18)	3/10 (30%)	3/13 (23%)	19/37 (51%)	0.178	2/12 (17%)	0.190
20q12	TOP1 (RP3-511B24)	2/10 (20%)	6/15 (40%)	22/36 (61%)	0.050	3/10 (30%)	0.320
High level amplifications							
1q32.1	MDM4 (RP11-563I16), PIK3C2B (RP11-739N20)	1/15 (7%)	0/17	5/38 (13%)	0.333	0/12	0.585
1q44	AKT3 (RP11-269F20, RP11-370K11)	0/15	0/16	1/41 (2%)	1.0	0/12	1.0
4q12	PDGFRA (RP11-231C18)	2/15 (13%)	0/16	2/40 (5%)	0.302	0/12	1.0
6p21.1	CCND3 (RP5-973N23, RP11-533O20)	0/15	0/17	0/41	-	0/12	-
7p22.1	PMS2 (RP11-90J23)	0/13	0/15	0/35	-	0/11	-
7p11.2	EGFR (RP5-1091E12, RP11-339F13)	10/15 (67%)	4/15 (27%)	21/33 (64%)	0.043	0/11	0.001

7q21.11	HGF (RP5-1098B1)	0/12	0/13	0/37	-	0/9	-
7q21.2	CDK6 (RP5-850G1)	0/14	0/11	0/39	-	0/11	-
7q31.2	MET (CTB-13N12)	0/11	0/14	0/35 (0%)	-	0/10	-
13q34	SOX1 (RP11-310D8)	0/15	0/16	1/41 (2%)	1.0	0/12	1.0
14q32.33	AKT1 (RP11-982M15)	0/12	0/14	0/29	-	0/9	-
19p13.3	STK11 (RP11-50C6)	0/12	1/15 (7%)	1/28 (4%)	1.0	0/11	1.0
19q13.31	XRCC1 (CTB-61I7, RP11-46C6, RP11-122E7)	0/15	0/17	0/39	-	0/12	-
19q13.32	ERCC2 (RP11-43E18)	0/10	0/13	0/37	-	0/12	-
20q12	TOP1 (RP3-511B24)	0/10	0/15	0/36		0/10	
Low- and high-level losses							
1p36.32	AJAP1 (RP11-319A11)	1/7 (14%)	6/12 (50%)	7/28 (25%)	0.258	3/8 (38%)	0.692
1p36.23	CAMTA1 (RP11-92O17, RP11-338N10)	4/15 (27%)	8/17 (47%)	11/38 (29%)	0.364	4/11 (36%)	1.0
1p32.3	CDKN2C (RP11-116M11)	1/12 (8.3%)	4/16 (25%)	9/36 (25%)	0.553	6/11 (55%)	0.058
1q42.12	PARP1 (RP11-15H13)	0/12	0/12	4/33 (12%)	0.476	0/10	1.0
6q26	PARK2 (RP11-30F7, RP11-1069J22)	3/13 (23%)	3/17 (18%)	8/36 (22%)	1.0	3/12 (25%)	0.718

9p23-p24.1	PTPRD (RP11-175E13, RP11-12I16)	7/14 (50%)	11/16 (69%)	14/41 (34%)	0.056	6/12 (50%)	0.765
9p21.3	CDKN2A/B (RP11-149I2)	13/15 (87%)	13/16 (81%)	35/41 (85%)	0.906	6/12 (50%)	0.013
10q23.31	PTEN (RP11-380G5)	15/15 (100%)	16/16 (100%)	39/40 (98%)	1.0	5/12 (42%)	<0.001
13q14.2	RB1 (RP11-305D15, RP11-174I10)	5/14 (36%)	6/16 (38%)	17/41 (42%)	0.946	3/12 (25%)	0.521
14q32.33	XRCC3 (RP11-73M18)	1/11 (9%)	2/14 (14%)	11/38 (29%)	0.362	6/10 (60%)	0.021
17p13.1	TP53 (P5-1030O14, RP11-199F11)	3/14 (21%)	6/16 (38%)	8/40 (25%)	0.379	5/12 (42%)	0.289
17q11.2	NF1 (RP11-1107G21, CTD-2370N5)	0/15	5/17 (29%)	8/41 (20%)	0.078	1/12 (8%)	0.681
19q13.31	XRCC1 (CTB-61I7, RP11-46C6, RP11-122E7)	1/15 (7%)	2/17 (12%)	7/39 (18%)	0.661	9/12 (75%)	<0.001
19q13.32	ERCC2 (RP11-43E18)	0/10	2/13 (15%)	8/37 (22%)	0.333	8/12 (67%)	0.001
22q12.3	TIMP3 (RP11-419C14, XXbac-677f7, RP11-616G18)	5/15 (33%)	9/17 (53%)	15/41 (37%)	0.472	4/12 (33%)	0.759
High-level losses							
1p36.32	AJAP1 (RP11-319A11)	0/7	0/12	0/28	-	0/8	-
1p36.23	CAMTA1 (RP11-92O17, RP11-338N10)	1/15 (7%)	0/17	1/38 (3%)	0.441	2/11 (18%)	0.087

1p32.3	CDKN2C (RP11-116M11)	0/12	0/16	0/36	-	0/11	-
1q42.12	PARP1 (RP11-15H13)	0/12	0/12	0/33	-	0/10	-
6q26	PARK2 (RP11-30F7, RP11-1069J22)	0/13	0/17	0/36	-	0/12	-
9p23-p24.1	PTPRD (RP11-175E13, RP11-12I16)	0/14	0/16	0/41	-	0/12	-
9p21.3	CDKN2A/B (RP11-149I2)	5/15 (33%)	9/16 (56%)	22/41 (54%)	0.382	3/12 (25%)	0.129
10q23.31	PTEN (RP11-380G5)	1/15 (7%)	1/16 (6%)	0/40	0.187	0/12	-
13q14.2	RB1 (RP11-305D15, RP11-174I10)	0/14	0/16	0/41	-	0/12	-
14q32.33	XRCC3 (RP11-73M18)	0/11	0/14	0/38	-	0/10	-
17p13.1	TP53 (P5-1030O14, RP11-199F11)	0/14	0/16	0/40	-	0/12	-
17q11.2	NF1 (RP11-1107G21, CTD-2370N5)	0/15	0/17	0/41	-	0/10	-
19q13.31	XRCC1 (CTB-61I7, RP11-46C6, RP11-122E7)	0/15	0/17	0/39	-	0/12	-
19q13.32	ERCC2 (RP11-43E18)	0/10	0/13	0/37	-	1/12 (8%)	0.167
22q12.3	TIMP3 (RP11-419C14, XXbac-677f7, RP11-616G18)	0/15	0/ 17	0/12	-	0/12	-

Supplementary Table 7. List of the 101 TCGA samples selected for validation purposes including only tumors reported as being *IDH1/2* wildtype or showing mesenchymal or classical transcription profiles.

Sample ID	Survival group	*IDH1* status*	Molecular subtype	Gender	Age at diagnosis (years)	Overall survival (days)
TCGA-06-0125	group A	wt	classical	female	64	1448
TCGA-08-0357	group A	wt	classical	male	50	1143
TCGA-06-0409	group A	na	mesenchymal	male	44	2152
TCGA-02-0085	group A	wt	mesenchymal	female	66	1325
TCGA-06-0164	group A	na	mesenchymal	male	48	1731
TCGA-08-0512	group A	na	mesenchymal	male	49	1282
TCGA-02-0025	group A	wt	mesenchymal	male	48	1300
TCGA-02-0069	group A	wt	proneural	female	31	1261
TCGA-08-0245	group A	wt	proneural	female	32	1151
TCGA-02-0269	group B	na	classical	male	69	327
TCGA-02-0333	group B	na	classical	female	78	133
TCGA-06-0402	group B	na	classical	male	71	8
TCGA-08-0511	group B	na	classical	male	69	235
TCGA-08-0514	group B	na	classical	female	70	337
TCGA-06-0145	group B	wt	classical	female	54	71
TCGA-02-0430	group B	na	classical	female	67	321
TCGA-08-0531	group B	na	classical	male	64	230
TCGA-06-0126	group B	wt	classical	male	87	211
TCGA-06-0148	group B	wt	classical	male	76	307
TCGA-06-0211	group B	wt	classical	male	48	360
TCGA-08-0246	group B	wt	classical	female	57	127
TCGA-06-0149	group B	na	mesenchymal	female	75	262
TCGA-06-0397	group B	na	mesenchymal	female	57	268

TCGA-02-0099	group B	wt	mesenchymal	male	47	103
TCGA-06-0645	group B	wt	mesenchymal	female	56	98
TCGA-02-0051	group B	na	mesenchymal	male	45	46
TCGA-02-0059	group B	na	mesenchymal	male	69	291
TCGA-02-0106	group B	na	mesenchymal	male	55	159
TCGA-02-0326	group B	na	mesenchymal	female	83	223
TCGA-06-0175	group B	na	mesenchymal	male	70	123
TCGA-06-0194	group B	na	mesenchymal	female	38	17
TCGA-06-0412	group B	na	mesenchymal	female	56	291
TCGA-08-0510	group B	na	mesenchymal	male	76	130
TCGA-02-0004	group B	wt	mesenchymal	male	59	345
TCGA-02-0086	group B	wt	mesenchymal	female	46	268
TCGA-02-0107	group B	wt	mesenchymal	male	57	211
TCGA-06-0122	group B	wt	mesenchymal	female	85	181
TCGA-06-0130	group B	wt	mesenchymal	male	54	358
TCGA-06-0143	group B	wt	mesenchymal	male	59	357
TCGA-06-0190	group B	wt	mesenchymal	male	63	317
TCGA-06-0197	group B	wt	mesenchymal	female	66	169
TCGA-06-0210	group B	wt	mesenchymal	female	73	225
TCGA-06-0644	group B	wt	mesenchymal	male	72	122
TCGA-08-0346	group B	wt	mesenchymal	male	70	256
TCGA-08-0352	group B	wt	mesenchymal	male	80	39
TCGA-08-0392	group B	wt	mesenchymal	male	60	14
TCGA-12-0620	group B	wt	mesenchymal	male	58	318
TCGA-06-0174	group B	wt	proneural	male	54	98
TCGA-06-0241	group B	wt	proneural	female	66	198
TCGA-06-0648	group B	wt	proneural	male	78	77

TCGA-08-0359	group B	wt	proneural	female	60	103
TCGA-08-0385	group B	wt	proneural	male	72	82
TCGA-02-0048	group B	wt	proneural	male	80	98
TCGA-02-0074	group B	wt	proneural	female	68	310
TCGA-06-0166	group B	wt	proneural	male	52	178
TCGA-06-0646	group B	wt	proneural	male	61	175
TCGA-02-0290	group C	na	classical	male	49	485
TCGA-02-0422	group C	na	classical	male	50	441
TCGA-02-0016	group C	wt	classical	male	50	859
TCGA-06-0187	group C	wt	classical	male	69	414
TCGA-08-0354	group C	wt	classical	female	53	546
TCGA-02-0285	group C	na	classical	female	50	422
TCGA-08-0355	group C	wt	classical	female	30	747
TCGA-02-0260	group C	na	classical	male	55	515
TCGA-02-0289	group C	na	classical	male	58	432
TCGA-02-0317	group C	na	classical	male	40	372
TCGA-08-0518	group C	na	classical	female	60	588
TCGA-08-0529	group C	na	classical	female	56	560
TCGA-02-0023	group C	wt	classical	female	38	612
TCGA-02-0070	group C	wt	classical	male	71	498
TCGA-02-0102	group C	wt	classical	male	44	372
TCGA-06-0137	group C	wt	classical	female	64	812
TCGA-08-0358	group C	wt	classical	male	50	678
TCGA-08-0375	group C	wt	classical	female	52	371
TCGA-02-0111	group C	na	mesenchymal	male	57	705
TCGA-02-0064	group C	wt	mesenchymal	male	49	600
TCGA-06-0124	group C	wt	mesenchymal	male	67	620

TCGA-12-0619	group C	wt	mesenchymal	male	60	1062
TCGA-08-0390	group C	wt	mesenchymal	male	69	425
TCGA-02-0337	group C	na	mesenchymal	male	48	764
TCGA-08-0509	group C	na	mesenchymal	male	64	383
TCGA-08-0522	group C	na	mesenchymal	male	61	635
TCGA-02-0039	group C	wt	mesenchymal	male	54	583
TCGA-02-0075	group C	wt	mesenchymal	male	64	635
TCGA-02-0079	group C	wt	mesenchymal	male	56	748
TCGA-06-0147	group C	wt	mesenchymal	female	51	541
TCGA-06-0152	group C	wt	mesenchymal	male	68	373
TCGA-06-0154	group C	wt	mesenchymal	male	55	424
TCGA-06-0176	group C	wt	mesenchymal	male	35	954
TCGA-06-0184	group C	wt	mesenchymal	male	64	907
TCGA-06-0189	group C	wt	mesenchymal	male	56	468
TCGA-08-0360	group C	wt	mesenchymal	male	76	468
TCGA-06-0139	group C	wt	mesenchymal	male	40	362
TCGA-08-0347	group C	wt	proneural	male	50	782
TCGA-08-0350	group C	wt	proneural	male	33	889
TCGA-08-0353	group C	wt	proneural	male	58	397
TCGA-02-0104	group C	wt	proneural	female	33	520
TCGA-06-0238	group C	wt	proneural	male	47	405
TCGA-08-0348	group C	wt	proneural	male	64	370
TCGA-12-0616	group C	wt	proneural	female	37	448
TCGA-12-0618	group C	wt	proneural	male	49	395